

Fractional quantum Hall effects in bilayers in the presence of inter-layer tunneling and charge imbalance

Michael R. Peterson¹, Z. Papić^{2,3,4} and S. Das Sarma¹

¹*Condensed Matter Theory Center, Department of Physics,
University of Maryland, College Park, MD 20742 USA*

²*Institute of Physics, University of Belgrade, Pregrevica 118, 11 000 Belgrade, Serbia*

³*Laboratoire Pierre Aigrain, Ecole Normale Supérieure,
CNRS, 24 rue Lhomond, F-75005 Paris, France and*

⁴*Laboratoire de Physique des Solides, Univ. Paris-Sud,
CNRS, UMR 8502, F-91405 Orsay Cedex, France*

(Dated: August 10, 2021)

Two-component fractional quantum Hall systems are providing a major motivation for a large section of the physics community. Here we study two-component fractional quantum Hall systems in spin-polarized half-filled lowest Landau level (filling factor $1/2$) and second Landau level (filling factor $5/2$) with exact diagonalization utilizing both the spherical and torus geometries. The two distinct two-component systems we consider are the true bilayer and effective bilayers (wide-quantum-well). In each model (bilayer and wide-quantum-well) we completely take into account inter-layer tunneling and charge imbalancing terms. We find that in the half-filled lowest Landau level, the FQHE is described by the two-component Abelian Halperin 331 state which is remarkably robust to charge imbalancing. In the half-filled second Landau, we find that the FQHE is likely described by the non-Abelian Moore-Read Pfaffian state which is also quite robust to charge imbalancing. Furthermore, we suggest the possibility of experimentally tuning from an Abelian to non-Abelian FQHE state in the second Landau level, and comment on recent experimental studies of FQHE in wide quantum well structures.

PACS numbers: 73.43.-f, 71.10.Pm

We theoretically investigate two-component spin-polarized fractional quantum Hall states in the bilayer half-filled first and second (first-excited) Landau levels considering the effects of both inter-layer tunneling and charge imbalance tunneling using exact diagonalization. The aspect that is different in this work compared to previous studies¹⁻⁵ is that we consider inter-layer tunneling along with charge imbalance tunneling. The reason we consider this *extra* tunneling term (charge imbalance), along with the an inter-layer tunneling term, is because recent experimental efforts^{6,7} have achieved bilayer FQHE systems where both the inter-layer and charge imbalance tunneling terms can be controlled by varying different system parameters (such as gate voltages) and a theoretical investigation of the physics of this system is both timely and important. Furthermore, the basic effects produced by a charge imbalance term in a theoretical exact diagonalization context is currently lacking. Before we delve into our results we provide an introduction, motivation, and historical perspective of this broad subject.

I. FRACTIONAL QUANTUM HALL EFFECT IN THE ONE- AND TWO-COMPONENT VARIETY

The fractional quantum Hall effect^{8,9} (FQHE) has proved to be the paradigm for emergent quantum physics for the nearly 30 years of its existence. It occurs when electrons are confined to a (quasi)-two-dimensional plane (such as in semiconductor structures,

e.g., GaAs/AlGaAs, with electron densities on the order of 10^{10} - 10^{11} cm^{-2}) and a strong perpendicular magnetic field is applied (usually on the order of tens of Tesla—sometimes up to ~ 40 T). Phenomenologically, the FQHE manifests as a quantized plateau in the Hall resistance R_{xy} (quantized to parts per billion) and a concomitant vanishing (or deep minimum that displays activated behavior) of the longitudinal resistance R_{xx} . The FQHE is said to occur at rational fractional filling factor ν when the quantized value of the Hall resistance is $R_{xy} = h/(\nu e^2)$, where $\nu = \rho/\phi_0$ (here ρ is the electron density and $\phi_0 = hc/eB$ is the magnetic flux quantum and B is the magnetic field strength, hence, ν is the number of electrons per magnetic flux quanta). The perpendicular magnetic field quantizes the two-dimensional kinetic energy into Landau levels separated in energy by $\hbar\omega_c = \hbar eB/mc$ and when the filling factor ν is made to be fractional (like it is for the FQHE), by either adjusting the electron density and/or magnetic field strength, the kinetic energy is a constant and completely flat bands obtain. In the limit that $\hbar\omega_c \rightarrow \infty$ (or the extreme quantum limit) the electron-electron Coulomb interaction is the dominant term in the Hamiltonian for electrons fractionally filling a Landau level (LL).

The one-component FQHE in the lowest orbital electronic Landau level is the most often discussed since it has been observed in the form of approximately 80 odd-denominator FQHE states and is well understood⁹⁻¹³. Essentially, the FQHE occurs due to the non-perturbative and electron-electron interaction driven formation of an emergent topologically ordered¹⁴ incom-

pressible quantum fluid at certain filling factors ν with non-zero energy gaps. This (bulk) energy gap, along with some sample disorder, explains the FQHE¹⁰.

Recently, the FQHE in half-filled Landau levels has reinvigorated the community due to its possible connection to topological quantum computing, non-Abelian quasiparticles, and the requisite cutting edge material science advances that have produced much of this new physics and continue to coax nature into revealing her secrets. In particular, the FQHE at filling factor $5/2$ ¹⁵, which corresponds to filling factor $1/2$ in the second orbital electronic Landau level, has arguably produced most of the excitement.

The denominator of ν for the “standard” fractional quantum Hall states is always odd and reflects the fermionic nature of the quasiparticles. At $\nu=1/(\text{even})$, naive, zeroth-order, theory asserts that no FQHE would be expected. This is because, at $\nu=1/(\text{even})$, the weakly interacting quasiparticles of the FQHE (Composite Fermions^{12,13}) experience a zero effective magnetic field and form a *gapless* exotic Fermi sea^{16–18}. In fact, no FQHE is experimentally observed in one-component systems at $\nu = 1/2$ instead showing signatures of the exotic Fermi sea^{19–21} (see Fig. 1).

The FQHE at $\nu = 2 + 1/2 = 5/2$ (the 2 comes from completely filling the spin-up and spin-down Landau levels) is particularly interesting and the only known and well established violator of the “odd-denominator” rule for the one-component FQH state with an even-denominator suggests some kind of interaction driven pairing among the weakly interacting emergent (quasi-)fermions and does not find a description within the standard FQHE theory. All FQHE states observed in the second Landau level (SLL), such as $5/2$, $7/3=2+1/3$, $8/3=2+2/3$, $12/5=2+2/5$, etc. (there are about 8 FQHE states observed in the SLL in all) are fragile when compared to the FQHE states in the lowest Landau level. The $5/2$ FQHE is one of the, if not the, strongest FQHE states in the SLL and yet has a measured activation gap only about 0.5 K or less. This is despite being measured in the world’s cleanest two-dimensional electron gas samples with mobilities over $30 \times 10^6 \text{ cm}^2/\text{Vs}$ at temperatures of less than 100 mK. Hence, there is a strong experimental drive to produce cleaner samples and apparatus capable of doing measurements at exceedingly low temperatures. Most early experimental observations of the FQHE at $5/2$ indicated the state to be one-component in nature^{22–29}. However, care needs to be taken when making broad absolute statements and there is some experimental evidence^{22,27,30} that puts the one-component interpretation of the $5/2$ FQHE into question, but, the interpretation of these results is notoriously difficult³¹.

Recently, the FQHE was observed³² at $\nu = 5/2$ in a low magnetic field where the ratio of the cyclotron energy $\hbar\omega_c$ to the Coulomb energy $e^2/\epsilon l$ (where e is the electron charge, ϵ is the dielectric constant of the host semiconductor and $l = \sqrt{\hbar/eB}$ is the characteristic length scale

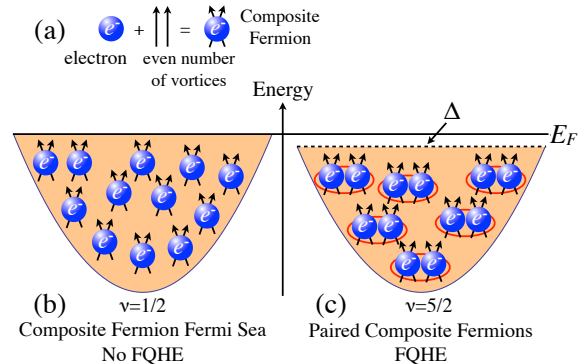


FIG. 1. (Color online) (a) A Composite Fermion is an electron bound (or attached) to an even number of quantum mechanical vortices of the many-body wavefunction, see Ref. 12 and 13. (b) A compressible Fermi sea of Composite Fermions forms for a one-component system at filling factor $\nu = 1/2$ in the lowest Landau level and produces *no FQHE* since a (Composite Fermion) Fermi sea has no energy gap. (c) In the half-filled second Landau level at $\nu = 5/2$ the electron-electron interaction is modified compared to the electron-electron interaction in the lowest Landau level (see text) causing the weakly interacting Composite Fermions to pair into a spin-polarized p -wave BCS state described by the Moore-Read Pfaffian wavefunction. This state, due to the quasiparticle pairing, has an energy gap and thus exhibits the FQHE.

called the magnetic length) is near unity or less. In that situation, it is not clear how the system would be completely spin-polarized and/or would not experience significant Landau level mixing. Recent experiments^{33–35} have begun to seriously tackle these two issues. Not surprisingly, theoretical groups have enthusiastically taken up the (considerable) challenge of understanding the role of Landau level mixing^{36–39}. That being said, the FQHE at $5/2$ has also been seen^{40,41} at magnetic field strengths of more than 10 T. A FQH state at fields that high is likely to be spin-polarized and, hence, one-component. Adding to the confusion is the fact that *all* theoretical work^{42,43} to date have established that, within a wide range of parameter space, the electrons are completely spin-polarized at $\nu = 5/2$. It is extremely difficult theoretically (computationally) to consider fully spin unpolarized FQHE and until there is definitive experimental evidence indicating the real system to be spin unpolarized we will theoretically consider the electron spin to be absolutely polarized throughout this work.

Arguably, the reason the FQHE at $5/2$ is so fascinating is its connection to topological quantum computing^{44,45}. An intriguing ansatz called the Moore-Read Pfaffian⁴⁶ is thought to describe the FQHE at $5/2$ and this ansatz has non-Abelian quasiparticle and quasihole excitations. It is proposed⁴⁷ that the world-lines of these non-Abelian excitations can be braided around each other, thus changing

the ground state in the degenerate manifold of ground states, and certain quantum computing gates can be achieved. This degenerate manifold of states is separated from the continuum by an energy gap that is topological in nature, since it is a FQHE state, thus, any sort of local disturbance to the system, like those caused from typical noise encountered in an experiment, will not be able to destroy the state due to its topological origin. Of course, if the disturbances are of an energy that is larger than the protective gap then the above does not hold. Using the non-Abelian quasiparticles and quasiholes of the Moore-Read (MR) Pfaffian (Pf) description of the $5/2$ state of the FQHE to achieve quantum computing gates that are topologically protected (called fault-tolerant topological quantum computation) is a major research goal⁴⁵. (Note that the non-Abelian quasiparticles that might exist for the FQHE at $5/2$ are so-called Ising anyons and are unable to be used for *universal* quantum computation—see Ref. 45 for more details on this point and how Ising anyons can be augmented to achieve a version of universal fault-tolerant topological quantum computation.)

Intuitively, the existence of the Moore-Read Pfaffian can be understood (see Fig. 1). Any time a Landau level is half-filled (not just at $\nu = 1/2$ as mentioned above but also at $\nu = 5/2 = 2 + 1/2$) naive zeroth-order theory tells us that a (Composite Fermion) Fermi sea^{16–18} can form. (Note that in this discussion we assume that the two completely filled Landau levels are inert which is the same as assuming that $\hbar\omega_c \rightarrow \infty$.) As is well known, any system of weakly interacting fermionic quasiparticles is unstable to pairing via the BCS^{48,49} pairing mechanism and, if the quasiparticles are spin-polarized, the simplest pairing is chiral p -wave symmetry ($p_x + ip_y$) (see the work by Read and Green in Ref. 50 for a discussion of the BCS mean field description of the FQHE in a half-filled Landau level.) The resulting paired state has an energy gap and the FQHE will occur as long as the system is clean enough and cold enough such and the Fermi energy lies within the FQHE gap. The Moore-Read Pfaffian wavefunction encapsulates this physics.

We briefly note that recently it has been pointed out^{51,52} that a competing state for the FQHE at $\nu = 5/2$ is the so-called anti-Pfaffian which is the particle-hole conjugate of the Moore-Read Pfaffian. The anti-Pfaffian is topologically distinct from the Pfaffian due to the fact that the two have different edge state behavior which, in principle, makes it possible to tell the two apart experimentally. We emphasize that both the Moore-Read Pfaffian and anti-Pfaffian *both* support non-Abelian quasi-hole and quasiparticle excitations so both could perform as platforms for fault-tolerant topological quantum computation. Whichever one happens to be responsible (if either) for the FQHE at $\nu = 5/2$ depends on how, and if, the particle-hole symmetry is broken⁵³ as well as experimental and material details such as disorder and Landau level mixing^{36–38}.

(All results in this work concerning the Pfaffian apply equivalently to the anti-Pfaffian within the constraints of

our approximation scheme since the model we use does not distinguish between Pfaffian and anti-Pfaffian. The reason for this is that our Hamiltonian is particle-hole symmetric, since we do not consider any particle-hole breaking terms such as those that might arise due to Landau level mixing. Since the Pfaffian and anti-Pfaffian are particle-hole conjugates of one another, their (bulk) physics, the subject of our current work, is identical.)

A natural question is why the FQHE is observed at $\nu = 5/2 = (2 + 1/2)$ and not, so far, at $\nu = 1/2$ for one-component systems. Theoretically, this is due to the physics of the lowest Landau level being different compared to the physics of the second Landau level^{54–57}, i.e., details matter. For the FQHE at filling factor $5/2$, the inert electrons in the lowest spin-up and spin-down Landau levels partially screen the electron-electron Coulomb interaction between the electrons half-filling the second Landau level—in fact, the electrons in the lower Landau level *over screen* the Coulomb interaction⁵⁶ which leads to a slight attraction among the quasiparticles causing them to form a BCS state—the Moore-Read Pfaffian state. Furthermore, the experimental details of a real quantum well—the single-electron wavefunction in the direction perpendicular to the two-dimensional surface has a finite extent (the so-called finite thickness of the quasi-two-dimensional electron system where typical experimental systems have widths ranging from approximately ~ 20 nm for the thinnest samples to ~ 60 nm for the wide-quantum-well samples) which produces subtle effects that make the effective interaction felt by the electrons in the half-filled second Landau level even more amenable to forming a non-Abelian Moore-Read Pfaffian FQHE at $\nu = 5/2$. Recently, it has been theoretically shown that (within certain approximate models) the effects of Landau level mixing^{36–38} might produce non-trivial and subtle effects that drive the system to the Pfaffian³⁷ or the anti-Pfaffian³⁸ state.

We reiterate that experimentally the FQHE at $\nu = 1/2$ has not been observed in *one-component systems* and theory^{4,58} suggests that it will not occur for a pure Coulomb interaction. However, one cannot rule out a Moore-Read Pfaffian FQHE at $\nu = 1/2$ if the system parameters are tuned in the perfect way^{59–61} or, perhaps, at extremely low temperatures not currently experimentally accessible.

However, about the same time the experimental observation of the $5/2$ FQHE was realized, the FQHE was also observed by Suen *et al.*^{62–64} and Eisenstein *et al.*⁶⁵ in the lowest Landau level at filling factor $\nu = 1/2$ in systems that were later determined by He *et al.*^{1–3} to be spin-polarized two-component systems. It turns out that the FQHE at $\nu = 1/2$ in two-component systems is described by the (Abelian) Halperin 331 two-component wavefunction⁶⁶. The system of Eisenstein⁶⁵ was an actual bilayer (two quasi-two-dimensional systems separated from one another by a tunneling barrier—typical parameters are quasi-two-dimensional electron systems of width ~ 20 nm separated from one another by a tunneling barrier of

thickness $\sim 3 - 10$ nm with electron densities on the order of 10^{11} cm^{-2}), thus, the two-components are the two layers. The FQHE at $\nu = 1/2$ in bilayers occurs by a two-part process where Laughlin⁹ states, at filling factor $1/3$, are formed in each layer and the fermions between layers form pairs. In the experiments by Suen *et al.*^{62–64} the electrons in the wide-quantum-well (a width of order ~ 70 nm and electron densities of $\sim 10^{11}$ cm^{-2}) minimize their single-particle energy by reorganizing into effectively two “layers” and, again, the FQHE at $\nu = 1/2$ occurs as described above. Recent observations^{6,7,67} of $\nu = 1/2$ and $1/4$ in wide-quantum-wells have rekindled interest in this rich system.

The discovery and identification of the FQHE at $\nu = 1/2$ was an exciting advance in the FQHE because it opened up the possibility of a new fractional quantum Hall state outside those given in the “standard” theory^{9,10,12,13}. However, the Halperin 331 state is closely related to the standard theory being that it is essentially a pairing of Laughlin states. Scarola and Jain⁶⁸ further generalized the Halperin 331 state to pairings of FQHE states belonging to the Jain sequence producing states for bilayer systems at filling factors other than $\nu = 1/2$ —they also produced *partially* pseudo-spin polarized states at $\nu = 1/2$ that are distinct from the Halperin 331 state.

Along with the recent observations^{6,7,67} of $\nu = 1/2$ and $1/4$ in wide-quantum-wells are observations^{6,7} of bilayer FQHE at filling factor $1/2$ in the lowest Landau level with *asymmetric* charge distributions—so-called “tilted samples”. A tilted sample is created by an additional charge gate that produces a charge asymmetry by “pushing” electrons from one side of the wide-quantum-well to the other. In the simplest approximation, this asymmetry produces a charge imbalance between one layer and the other while keeping the total filling factor ν fixed. That is, the individual filling factors in each layer, ν_1 and ν_2 , respectively, (keeping $\nu_1 + \nu_2 = \nu$ fixed) can be varied between $(\nu_1, \nu_2) = (\nu, 0)$, to $(\nu_1, \nu_2) = (\nu/2, \nu/2)$, to $(\nu_1, \nu_2) = (0, \nu)$.

Of course, care should be taken when considering the effects of a charge gate that presumably causes charge asymmetry in a wide-quantum-well. Recently, Scarola *et al.*⁶⁹ have used the local-density-approximation (LDA) to get a more realistic handle on exactly what tilting does to the charge distribution and relative single-electron energy levels in the quantum well. They went on to analyze the system with the use of variational wavefunctions finding that the recent experimental observation of the FQHE at $\nu = 1/2$ by Shabani *et al.*⁷ at intermediate charge imbalancing is likely described by a partially pseudo-spin polarized bilayer state^{68,69}.

The purpose of the present work is to understand the general effects of charge imbalancing in the most minimal model one can consider to describe the bilayer FQHE in an exact context—that is, using exact diagonalization. Our work compliments recent work⁶⁹ since we are solving the Hamiltonian exactly instead of using a combination of LDA and variational wavefunctions. As such, we are

restricted to only certain ansatz, namely the Moore-Read Pfaffian and the Halperin 331 state. We emphasize that our solution is general and exact.

In Sec. II we present our theoretical model in the form of a Hamiltonian that can describe either a true bilayer and effective (wide-quantum-well) bilayer where we consider both inter-layer and charge imbalance tunneling terms. Four (two plus two) variational states are discussed in Sec. III that are thought to describe our bilayer and effective bilayer Hamiltonian. Secs. IV and V present our results for the bilayer and wide-quantum-well model in both the lowest Landau level (in both the spherical and torus geometry) and second Landau level (in the spherical geometry). Finally, in Sec. VI, we present our conclusions.

II. THEORETICAL MODELS: TRUE BILAYER AND EFFECTIVE BILAYER

There are two experimental systems in which two-component FQHE systems can be produced. One of them is to manufacture a true bilayer system which consists of two parallel (quasi-)two-dimensional electron systems of width w separated from one another by a tunneling barrier of thickness d . This system is used extensively by the Eisenstein group at CalTech⁶⁵ and is what one generally thinks about when contemplating a bilayer system. The height of the barrier can be adjusted such that electrons are either localized in separate layers or delocalized between the two layers, i.e., large energetic barrier or small energetic barrier, respectively. In other words, the symmetric-anti-symmetric energy gap, Δ_{SAS} , can be controlled independently of the individual well width w and the layer separation d . In this system, an electron can be in the right (R) or left (L) state, written as $|R\rangle$ or $|L\rangle$, respectively. Fig. 2 shows a schematic diagram of a bilayer system consisting of two parallel two-dimensional electron systems where the electrons in each layer are confined to two-dimensions by a quantum well of width w (both layers have the same width) and the quantum-well-center to quantum-well-center separation is d ($d \geq w/2$). A typical density profile of electrons in the right or left layer ($\langle R|R\rangle$ or $\langle L|L\rangle$) is also shown in Fig. 2a. The ground state of the single-electron bilayer Hamiltonian is the symmetric state S given by

$$|S\rangle = \frac{|R\rangle + |L\rangle}{\sqrt{2}} \quad (1)$$

and the next higher energy state is the anti-symmetric state given by

$$|AS\rangle = \frac{|R\rangle - |L\rangle}{\sqrt{2}} \quad (2)$$

(assuming no charge imbalance term in the Hamiltonian). The two states (S and AS) are separated by an energy difference Δ_{SAS} and their respective (typical) density profiles ($\langle S|S\rangle$ and $\langle AS|AS\rangle$) are shown in Fig. 2b.

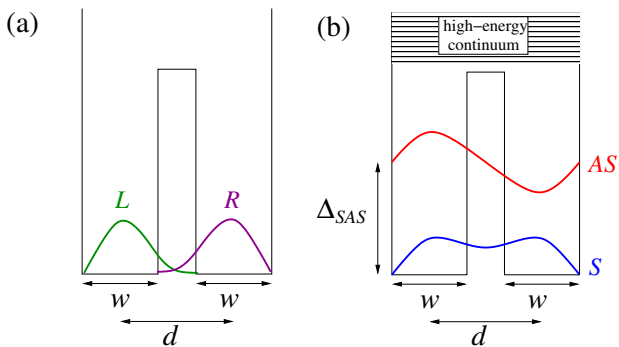


FIG. 2. (Color online) A bilayer system consisting of two (quasi-)two-dimensional quantum wells of width w separated from one another by d ($d \geq w/2$). (a) Typical density profile of an electron localized in either the right (R) or left (L) layer, respectively. (b) The ground state single particle wavefunction (the symmetric (S)) state and the next higher energy state (the anti-symmetric (AS)) state separated in energy from one another by the so-called symmetric-anti-symmetric energy gap Δ_{SAS} .

The other way to experimentally create a two-component FQHE system is to make a single (quasi-)two-dimensional electron gas of large width, a so-called wide-quantum-well (WQW), as done by the Shayegan group at Princeton^{6,7,62–64}. In this case, the electrostatic inter-

action between the electrons (at the Hartree-Fock level) compels the system to behave as an effective bilayer. The electron density for the ground state is maximum (and symmetric) near the edges of the wide-quantum-well and depleted in the middle. The energy level diagram and typical density profiles are similar to those shown in Fig. 3a. Note that in this system, Δ_{SAS} is a strong function of the width W (and electron density) of the wide-quantum-well. This contrasts the bilayer system described above where, in principle, Δ_{SAS} , the individual well width w , and the layer separation d can all be independently adjusted.

A simplified model for the WQW is due to Papić *et al.*⁴ where the ground state of a wide-quantum-well of width W is taken to be a symmetric state (for example, $\langle z|S\rangle \sim \sin(\pi z/W)$) and the next excited state an anti-symmetric state (for example, $\langle z|AS\rangle \sim \sin(2\pi z/W)$)—both the S and AS states are written on the interval $z \in [0, W]$. (The coordinates of the (quasi-)two-dimensional plane will always be denoted by x and y and the coordinates of the wide-quantum-well width, bilayer layer separation, or individual quantum-well thickness will be denoted by z .) The density profiles for the WQW model are shown in Fig. 3b. In this model, one can transform to the layer-basis (right and left layers) by taking $|L\rangle = (|S\rangle + |AS\rangle)/\sqrt{2}$ and $|R\rangle = (|S\rangle - |AS\rangle)/\sqrt{2}$, cf. Fig. 3.

The Hamiltonian for our two-component model systems can be written (in the SAS -basis) as

$$H = \frac{1}{2} \sum_{\{m_i, \sigma_i = S, AS\}} \langle m_1 \sigma_1, m_2 \sigma_2 | V | m_3 \sigma_3, m_4 \sigma_4 \rangle c_{m_1 \sigma_1}^\dagger c_{m_2 \sigma_2}^\dagger c_{m_3 \sigma_3} c_{m_4 \sigma_4} \delta_{m_1+m_2, m_3+m_4} - \frac{\Delta_{SAS}}{2} \sum_m (c_{mS}^\dagger c_{mS} - c_{mAS}^\dagger c_{mAS}) + \frac{\Delta\rho}{2} \sum_m (c_{mS}^\dagger c_{mAS} + c_{mAS}^\dagger c_{mS}). \quad (3)$$

The second to last term (the term with the prefactor $\Delta_{SAS}/2$) controls inter-layer tunneling and, in the SAS -basis is represented by the pseudo-spin operator \hat{S}_z , while the last term (prefactor $\Delta\rho/2$) controls charge imbalance and is represented by the pseudo-spin operator \hat{S}_x . In our convention, positive $\Delta\rho$ drives the electrons into the right (R) layer. Notice that $\langle m_1 \sigma_1, m_2 \sigma_2 | V | m_3 \sigma_3, m_4 \sigma_4 \rangle$ is different in the bilayer case than it is in the WQW case, in general. Namely, in the bilayer case, the Coulomb matrix element is found by using the transformations given in Eqs. 1 and 2 and the fact that the potential energy between two electrons a distance r apart in a given layer (the right layer, say) of width w is given by the Zhang-Das Sarma⁷⁰ potential $V_{\text{intra}}(r) = 1/\sqrt{r^2 + w^2}$ and the potential between two electrons in two different layers separated by a distance d is given by $V_{\text{inter}}(r) = 1/\sqrt{r^2 + d^2}$. In the WQW system the Coulomb matrix element is calculated by considering the wavefunctions for the S and AS states ($\langle z|S\rangle$ and $\langle z|AS\rangle$) and doing the required integrals.

In the (left/right) layer-basis we can write the bilayer Hamiltonian very simply as

$$\hat{H} = \sum_{i < j} [V_{\text{intra}}(|\mathbf{r}_i - \mathbf{r}_j|) + V_{\text{intra}}(|\tilde{\mathbf{r}}_i - \tilde{\mathbf{r}}_j|) + V_{\text{inter}}(|\mathbf{r}_i - \tilde{\mathbf{r}}_j|)] - \Delta_{SAS} \hat{S}_x + \Delta\rho \hat{S}_z, \quad (4)$$

where operators \hat{O} with a tilde are written in the layer-basis and coordinates \mathbf{r} and $\tilde{\mathbf{r}}$ belong to electrons in different layers. Switching from the layer- to the SAS -basis is a pseudo-spin rotation. Note that for $d = 0$ the Hamiltonian is symmetric between Δ_{SAS} and $\Delta\rho$. Increasing d destroys this symmetry and it becomes harder to drive the system to be one-component in the layer-sense.

In all of our results we use the *natural* FQHE units:

lengths are given in units of the magnetic length l and

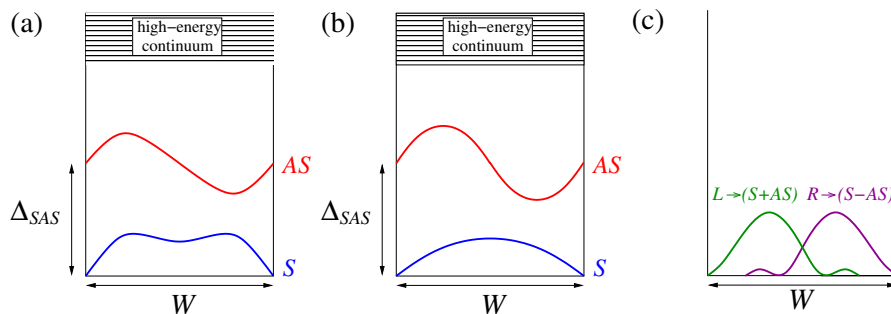


FIG. 3. (Color online) (a) A two-component system created by a wide-quantum-well (WQW). The electrostatic potential generated by the electrons self-consistently creates an effective bilayer system by pushing the electrons towards the walls of the WQW. Note that (a) is *not* identical to Fig. 2b even though they are very similar—specifically, Δ_{SAS} is a strong function of W and the electron density in WQW systems as opposed to bilayers. (b) The model of Papić *et al.*⁴ which can be transformed into the layer-basis shown in (c).

energies are given in units of the Coulomb energy $e^2/\epsilon l$.

(Note that the system we are considering is a rather general two-component Hamiltonian and when the layer separation is zero any results we find are applicable to SU(2) symmetric two-component systems where the constituents interact by a Coulomb-like interaction—exactly Coulombic for the lowest Landau level and a slightly modified Coulombic interaction for the second Landau level. For example, when $d = 0$ the Hamiltonian (Eq. 3) describes spin-full electrons interacting via a Coulomb interaction with both \hat{S}_z and \hat{S}_x terms.)

III. VARIATIONAL WAVEFUNCTIONS: MOORE-READ PFAFFIAN AND HALPERIN 331

We consider four variational wavefunctions to describe our FQH system for half-filled lowest and second Landau levels ($\nu = 1/2$ and $\nu = 5/2$, respectively) even though it will appear at first that we are only considering two. Namely, we consider the one-component Moore-Read Pfaffian⁴⁶ (Pf) and two-component Halperin 331 (331) wavefunctions⁶⁶. (Note that work^{71–77} has been done on the FQHE at total filling factor of unity, i.e., $\nu = 1/2 + 1/2 = 1$, however, that is not the case that we study in this work.)

The Moore-Read Pfaffian state is written as

$$\Psi_{\text{Pf}} = \text{Pf} \left\{ \frac{1}{z_{i,a} - z_{j,a}} \right\} \prod_{i < j}^N (z_{i,a} - z_{j,a})^2 \quad (5)$$

where $z_{i,a} = x_{i,a} - iy_{i,a}$ is the position of the i th electron in complex coordinates with a labeling its state, i.e., $a = S, AS, R$ or L . The origin of this wavefunction can be understood at an intuitive level. If one writes down an ansatz wavefunction to describe a BCS paired state of Composite Fermions in a half-filled Landau level then one arrives at a wavefunction of the Pfaffian form⁷⁸, i.e.,

$$\text{Pf}\{g(r_{ij})\} \prod_{i < j} (z_i - z_j)^2 =$$

$$\mathcal{A}\{g(r_{12})g(r_{34}) \dots g(r_{N-1,N})\} \prod_{i < j} (z_i - z_j)^2 \quad (6)$$

where $g(|\mathbf{r}_i - \mathbf{r}_j|)$ is the real space pairing amplitude for a pair of electrons located at position \mathbf{r}_i and \mathbf{r}_j , $\prod_{i < j} (z_i - z_j)^2$ binds two quantum mechanical vortices of the many-body wavefunction to each electron (the Composite Fermion transformation and fixes the filling factor in a Landau level to $1/2$). \mathcal{A} is the anti-symmetrization operator.

Despite the intuitive picture that goes along with the Moore-Read Pfaffian wavefunction it was originally derived using conformal field theory and, as such, the Pf has a low-energy effective conformal field theory description, cf. Refs. 46, 79 and 50. It is within this conformal field theory that the understanding of the non-Abelian nature of the quasiparticle excitations was first illuminated. However, whether or not the Pf has anything to do with the physics of the FQHE at $5/2$ has depended crucially on numerical calculations and comparisons with the results of exact diagonalization^{42,43,58–61,80}. As mentioned above, the details matter greatly in determining the physics of the FQHE at $5/2$, such as, finite thickness effects^{59,60}, the competition between FQHE states and non-FQHE striped phases⁸⁰ and the compressible (Composite Fermion) Fermi sea^{16,17} (as mentioned, the latter occurs in the lowest Landau level at $\nu = 1/2$ while the former occurs in the second Landau level at $\nu = 5/2$), the effects of Landau level mixing^{36–38}, etc. Note that most of the numerical studies mentioned above do not treat the $\nu = 5/2$ problem in full complexity, i.e. with the lowest Landau level filled with two spin species and one Landau level half filled. Instead, because of computational simplicity, one considers a half filled lowest Landau level (usually without spin) with an effective interaction that contains the form factors of the first excited Landau level—the appropriate Haldane pseudopotentials⁸¹. This is what we mean by “ $\nu = 5/2$ in an exact diagonalization context.

Thus, it should be clear that any effective conformal

field theory (or effective BCS mean field Hamiltonian⁵⁰) written down to describe the physics at $5/2$ is only as good as its physical predictions and agreement with experiments *and* its agreement with numerical calculations. This is because the entire reason for the existence of the FQHE at all filling factors is due to non-perturbative physics arising from the strongly interacting electrons interacting with a Coulomb interaction modified by the details of which Landau level is fractionally filled by electrons, the thickness the quantum well, the amount of Landau level mixing that is taking place, etc. Hence, any mean field theory that throws away all these details at the first step cannot explain, for example, why the FQHE occurs at $\nu = 5/2$ and not $\nu = 1/2$ (or for that matter, at $9/2$ or $13/2$...) without the aid of both numerical calculations and, most importantly, experiments. In the end, whether a particular candidate wavefunction, e.g. Moore-Read Pfaffian or Laughlin or Halperin 331 or Composite Fermion states, etc., describes a real FQHE at some filling factor is an energetic question delicately depending on competing states where all the details of the microscopic Hamiltonian may eventually matter, and therefore, extreme caution is necessary in identifying experimental FQHE states with candidate incompressible wavefunctions, particularly in higher LLs and/or multi-component systems where various competing states are, in general, more viable.

The Halperin (two-component) 331 wavefunction is written as

$$\Psi_{331} = \prod_{i < j}^{N/2} (z_{i,1} - z_{j,1})^3 \prod_{i < j}^{N/2} (z_{i,2} - z_{j,2})^3 \prod_{i,j}^N (z_{i,1} - z_{j,2}), \quad (7)$$

where the subscript 1 (or 2) on $z_{i,1}$ labels the quantum number of the electron. This quantum number could describe spin (up or down), layer (R or L), subband (S or AS). Note that in our work, we consider the bilayer situation so the subscript will either denote the layer or the symmetric or anti-symmetric state depending on in which basis we choose to work. Intuitively, the origin of this wavefunction is that, in a bilayer system in a half-filled Landau level, the electrons form $\nu = 1/3$ Laughlin states⁹ ($\prod_{i < j}^N (z_i - z_j)^3$) among each electron component and then pair among different components (simple Jastrow factor $\prod_{i,j}^N (z_{i,1} - z_{j,2})$).

(Note that we always drop the Gaussian factors ($\sim \exp(-\sum_i |z_{i,a}|^2)$) that are always present when writing wavefunctions describing electrons entirely in (or projected into) the lowest Landau level—in fact, the Gaussian is often considered to be part of the measure so one is technically not “dropping” anything at all.)

It is important to realize that the Moore-Read Pfaffian is a one-component state that can be one-component in both the SAS -basis sense or in the layer-basis sense, see Fig. 4a and 4b. That is, the Pf wavefunction either describes pairing among one-component electrons in the

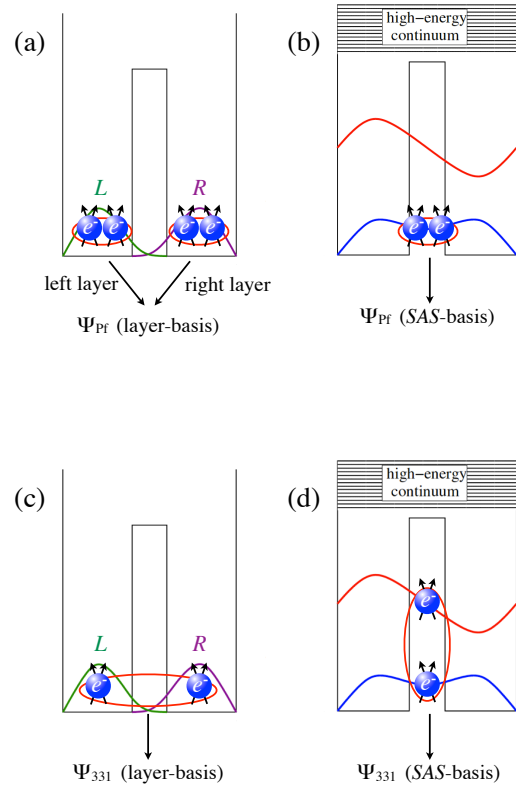


FIG. 4. (Color online) The Moore-Read Pfaffian wavefunction written in the (a) layer- and (b) SAS -basis where the p -wave pairing in the former is between Composite Fermions in the right (or left) layer and the p -wave pairing in the SAS -basis is between electrons in the symmetric (S) state. The Halperin 331 state is shown in (c) the layer-basis and (d) the SAS -basis where in the layer-basis the 331 state pairs Composite Fermions between layers and in the SAS -basis it pairs Composite Fermions in the symmetric (S) and anti-symmetric (AS) states.

right (R) layer or left (L) layer (the layer-basis) or pairing among one-component electrons in the symmetric (S) state (the SAS -basis). The former is the Pfaffian state that has its origin in the single-layer FQHE, while the latter is the Pfaffian understood as the even (symmetric) channel of the BCS description by Read and Green⁵⁰. (We choose our charge imbalancing term to drive the electrons into the right layer, however, we could have equivalently chosen the charge imbalance term to drive the electrons into the left layer.) Thus, there are actually *two* Moore-Read Pfaffian states to consider when both tunneling terms (Δ_{SAS} and $\Delta\rho$) are non-zero (or three if we allow the sign of $\Delta\rho$ to change). When the system is $SU(2)$ symmetric, i.e., when the layer separation is zero, the two different states are simply related via a rotation

in pseudo-spin space.

The Halperin 331 state can also be two-component in two ways: it can describe pairing of electrons in the R and L layers (the layer-basis) or it can describe pairing of electrons in the S and AS states (the SAS -basis), see Fig. 4c and Fig. 4d. Hence, there are *two* Halperin 331 states to consider when both tunneling terms are finite. Note, however, that the Halperin 331 state, as usually understood, is defined in the layer-basis. Again, in the $SU(2)$ situation, these two 331 states are related via a pseudo-spin rotation.

Thus, instead of dealing with two variational wavefunctions (Pf and 331) we are dealing with four—two Pfs and two 331s. Even though the two pairs of wavefunctions are related via a pseudo-spin rotation, when the $SU(2)$ symmetry is broken this is no longer the case and the determination of which state describes the physics is non-trivial.

In our calculations we utilize the spherical geometry⁸¹ where the electrons are confined to the surface of a sphere of radius $\sqrt{N_\phi}/2$ and a radial magnetic field (perpendicular to the surface) is produced by a magnetic monopole of strength $N_\phi/2$ placed at the center. (We briefly consider the torus geometry below.) The total magnetic flux piercing the surface is N_ϕ and is either an integer or half-integer according to Dirac⁸². The filling factor (in the partially filled Landau level) is given by $\lim_{N \rightarrow \infty} N/N_\phi$ for N electrons. In our case, we are considering the Moore-Read Pfaffian and Halperin 331 states which describe a half-filled Landau level, thus, the relationship between N and N_ϕ for a finite spherical system is $N_\phi = 2N - 3$. Due to computational constraints we consider $N = 8$ and $N_\phi = 13$ (the $N = 6$ particle system is aliased with a $2/3$ filled Landau level and, thus, produces ambiguous results and the $N = 10$ electron system is too big to consider while adequately exploring the large parameter space inherent when tackling a two-component Hamiltonian with both inter-layer and charge imbalancing tunneling). In the spherical geometry, possible FQHE states are uniform states with total angular momentum $L = 0$.

In this work we consider the overlap between the exact ground state of the model Hamiltonian and the four variational states: (1) Pf in the SAS -basis, (2) Pf in the layer-basis, (3) 331 in the SAS -basis and (4) 331 in the layer-basis.

IV. RESULTS: LOWEST LANDAU LEVEL

We first present our results for the lowest Landau level where we consider (i) the wavefunction overlap between the four variational states (Pf in the layer- and SAS -basis and the 331 in the layer- and SAS -basis) and the exact ground state of the Hamiltonian—note that since all the variational states describe the FQHE they have $L = 0$ and so if the exact ground state of the Hamiltonian does not also have total angular momentum $L = 0$

the overlaps will be trivially zero since they are then of different symmetry. (ii) the pseudo-spin expectation values of the exact ground state, which is more descriptively referred to as the expectation value of $(N_S - N_{AS})/2$ or $(N_R - N_L)/2$ where N_S , N_{AS} , N_R and N_L are the expectation values of the number of electrons in the symmetric state, the anti-symmetric state, the right layer and the left layer, respectively. Alternatively, this is simply $\langle \hat{S}_z \rangle$ and $\langle \hat{S}_x \rangle$ in the SAS -basis, but we prefer to use the more physical $(N_S - N_{AS})/2$ and $(N_R - N_L)/2$ since this does not depend on the basis in which we choose to write the Hamiltonian. (iii) the FQHE energy gap which is *defined* here as the energy difference between the $L = 0$ ground state and the first excited state (this is often times referred to as the “neutral gap” but we will call it the FQHE gap throughout this work) and, lastly, (iv) we investigate the energy spectra in the torus geometry. We show all of these quantities from a variety of vantage points to give the clearest picture of the physics since things can get complicated rather quickly with so many parameters in the Hamiltonian, namely, layer separation d or WQW width W , SAS energy gap Δ_{SAS} and the charge imbalancing gap $\Delta\rho$.

A. Bilayer

We first present our results for the bilayer Hamiltonian. Fig. 5a shows the overlap between the Moore-Read Pfaffian and the exact ground state in the layer-basis (left column) and SAS -basis (right column) as a function of Δ_{SAS} and $\Delta\rho$ for values of layer separation d ranging from $d = 0.05$ to 6. For the layer-basis (left column), it is clear that increasing Δ_{SAS} does not drive the system into the Pf phase, i.e., it does not increase the overlap between the layer-basis Pf with the exact ground state. However, increasing the charge imbalance $\Delta\rho$ does drive the system into the Pf phase. For increasing values of d it takes a larger value of $\Delta\rho$ to produce a ground state with a high overlap with the layer-basis Pf. This behavior is easy to understand. Non-zero $\Delta\rho$ makes the system one-component in the layer-sense and thus a layer-basis Pf wavefunction (which is a one-component wavefunction) has a large overlap. It is also understandable that finite layer separation d would make it harder to polarize the electrons in the layer-sense, i.e., the electrons prefer to remain two-component so they can take advantage of the reduction in potential energy between electrons in neighboring layers (the interaction is $1/\sqrt{r^2 + d^2}$ as opposed to $1/r$ for electrons in the same layer).

The overlap between the exact ground state and the Moore-Read Pfaffian in the SAS -basis shows essentially the opposite behavior. This time, non-zero Δ_{SAS} drives the system to be one-component. Notice that for the smallest value of layer separation $d = 0.05$ the system is nearly $SU(2)$ symmetric and the two bases (layer and SAS) are (nearly) pseudo-spin rotations of each other. The figure is deceptive because the scale on the two axes

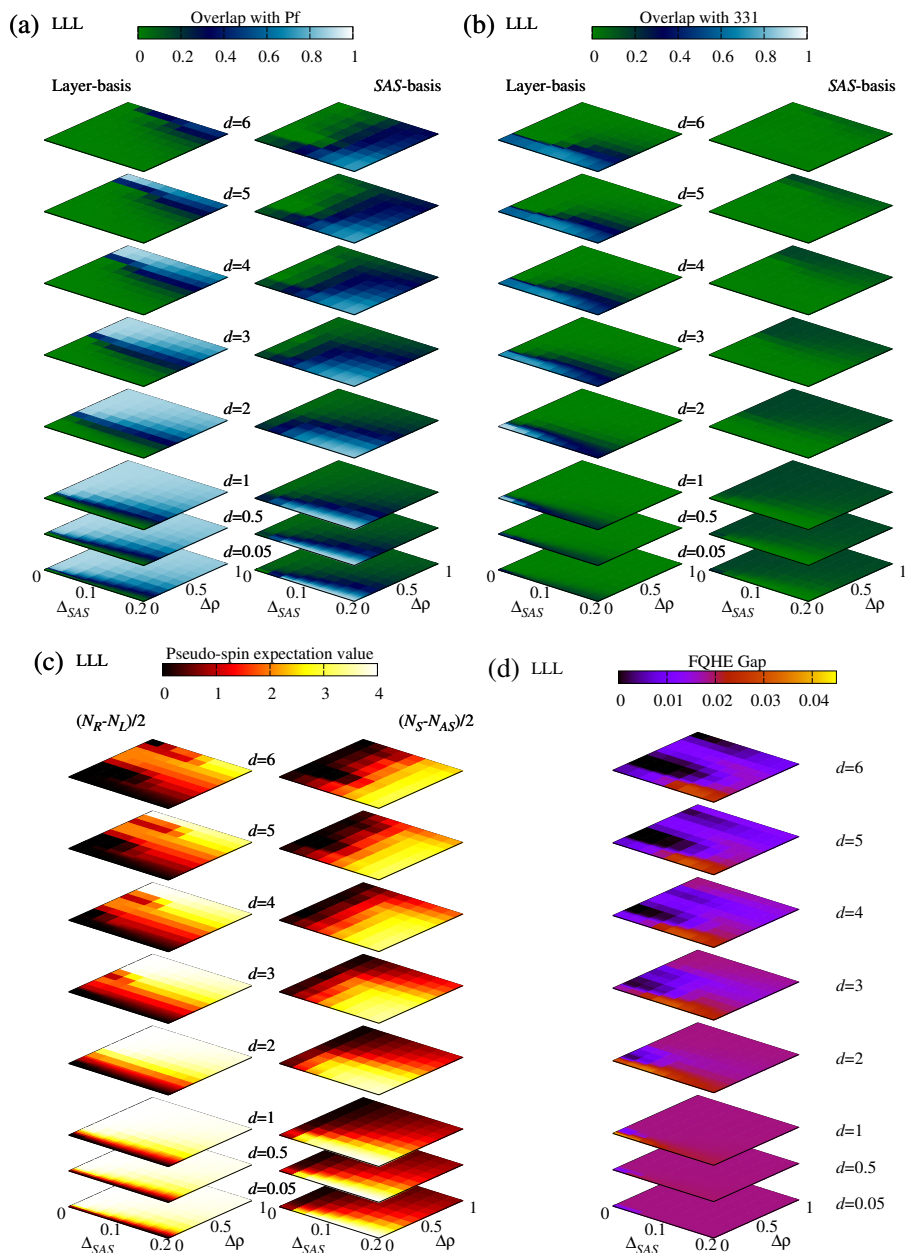


FIG. 5. (Color online). Lowest Landau level: (a) Wavefunction overlap between the exact ground state of the bilayer Hamiltonian and the Moore-Read Pfaffian written in the layer-basis (left column) and the *SAS*-basis (right column) shown as a function of inter-layer tunneling Δ_{SAS} and charge imbalance $\Delta\rho$ for different values of layer separation d and zero individual layer thickness $w = 0$. (b) Same as (a) but for the Halperin 331 wavefunction. (c) Pseudo-spin expectation value or, more physically, the expectation value of $(N_R - N_L)/2$ (left column) and $(N_S - N_{AS})/2$ (right column) as a function of Δ_{SAS} and $\Delta\rho$. (d) shows the FQHE (neutral) energy gap for the exact bilayer Hamiltonian.

is different, but the two figures are essentially identical upon reflection across the $\Delta_{SAS} = \Delta\rho$ line. This symmetry is quite obviously destroyed upon increasing d .

A naive look at Fig. 5a would lead to a conclusion that we have found the Pfaffian state in some regions of $\Delta_{SAS} - \Delta\rho$ phase diagram. The reader may wonder how robust these conclusions are with increasing system size. Although we are unable to calculate the full phase

diagram for $N = 10$ electrons, we can gain insight into the limiting cases when either $\Delta\rho$ or Δ_{SAS} is very large. If we work in the layer-basis and $\Delta\rho$ is very large, we recover the single-layer physics; for our system of $N = 8$ electrons, it turns out⁶¹ that the ground state for the lowest Landau level Coulomb interaction is already in the universality class of Moore-Read Pfaffian. However, this no longer holds for larger systems such as $N = 10$

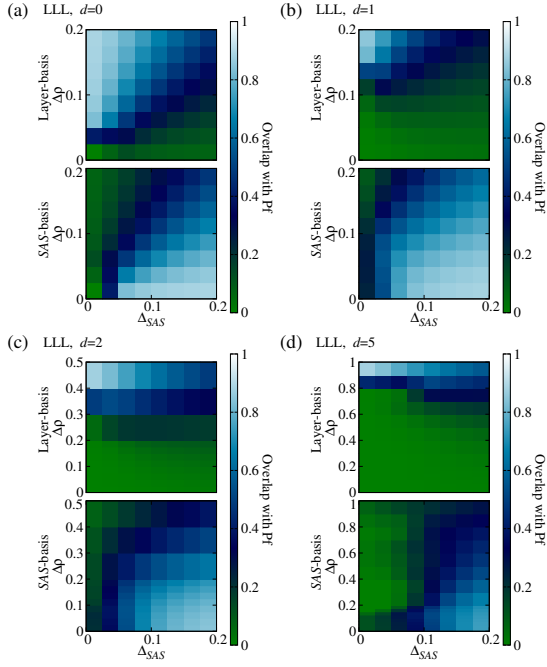


FIG. 6. (Color online) Lowest Landau level: Wavefunction overlap between the Moore-Read Pfaffian wavefunction in the layer-basis (top panel) and the SAS -basis (lower panel) and the exact ground state for (a) $d = 0$, (b) $d = 1$, (c) $d = 2$ and (d) $d = 5$.

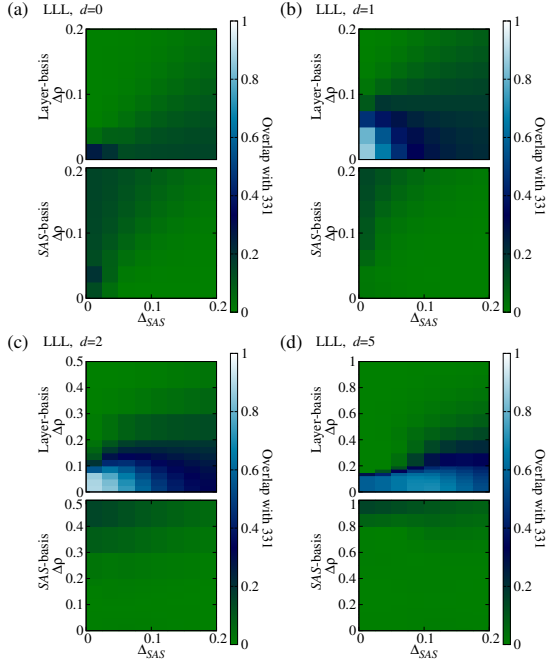


FIG. 7. (Color online) Lowest Landau level: Wavefunction overlap between the Halperin 331 wavefunction in the layer-basis (top panel) and the SAS -basis (lower panel) and the exact ground state for (a) $d = 0$, (b) $d = 1$, (c) $d = 2$ and (d) $d = 5$.

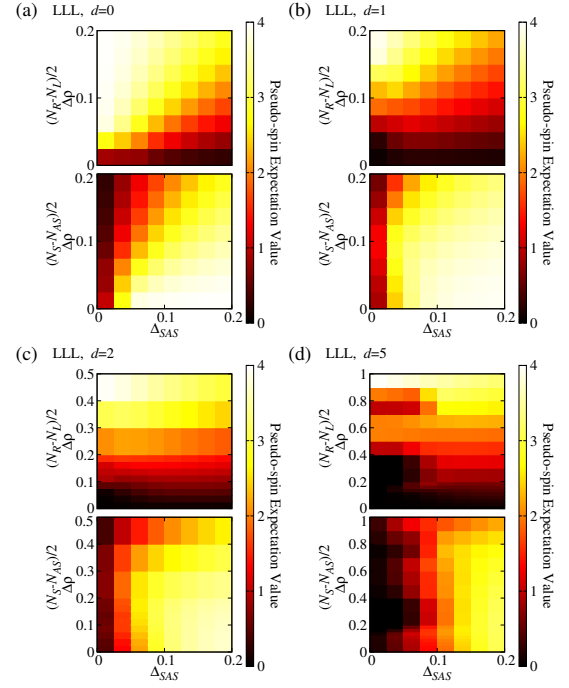


FIG. 8. (Color online) Lowest Landau level: (Pseudo-spin) expectation value of the exact ground state of $(N_R - N_L)/2$ (top panel) and $(N_S - N_{AS})/2$ (lower panel) for (a) $d = 0$, (b) $d = 1$, (c) $d = 2$ and (d) $d = 5$. Note that these figures (especially for $d = 0$) are qualitatively similar to our cartoon schematic in Fig. 10 since the pseudo-spin expectation value essentially describes the one- or two-component nature of the ground state. Also, finite d breaks the $SU(2)$ symmetry of reflection across the $\Delta_{SAS} = \Delta\rho$ line assumed in Fig. 10.

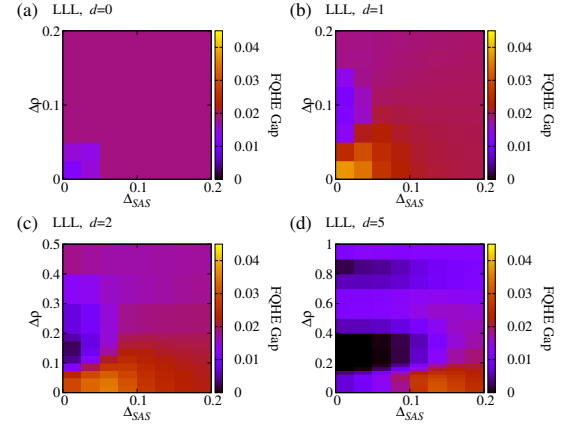


FIG. 9. (Color online) Lowest Landau level: FQHE energy gap for (a) $d = 0$, (b) $d = 1$, (c) $d = 2$ and (d) $d = 5$.

and $N = 12$, leading to the conclusion that high overlaps with the Pfaffian in the layer-basis in Fig. 5a are a finite size effect for $\nu = 1/2$. On the other hand, if we work in the SAS -basis and increase Δ_{SAS} , all the electrons will occupy the symmetric subband. This is again a one-component system, but with the interaction slightly softened with respect to pure Coulomb⁸³. It is

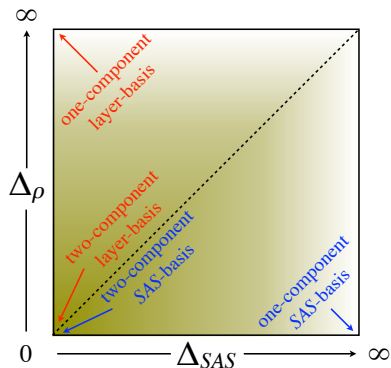


FIG. 10. (Color online) By varying either Δ_{SAS} or $\Delta\rho$ the system can be two-component (in the *SAS*-basis or layer-basis sense) when Δ_{SAS} and $\Delta\rho$ are small and one-component (again in either the *SAS*-basis or layer-basis sense) for large values of either Δ_{SAS} or $\Delta\rho$. The shading qualitatively indicates the one-component to two-component nature of the system with the darker shade indicating a two-component system and the lighter color a one-component system.

known⁶¹ that softening the Coulomb interaction via various finite-width corrections can lead to a phase transition between compressible and incompressible (non-Abelian) states, but this also leads to a significant reduction of the gap (as we show below). Therefore, the Pfaffian which is seen in our data for *SAS* basis is also not a typical incompressible state, but rather a “critical” state with some Pfaffian correlations and a small gap. In the remainder of this section, we will nonetheless, for the sake of brevity, refer to the one-component phase (fully polarized by either Δ_{SAS} or $\Delta\rho$) as described by the appropriate basis “Pfaffian” state, cautioning the reader that such a designation most likely does not survive in the thermodynamic limit.

Next we consider the overlap between the exact ground state and the Halperin 331 state in the layer-basis (left column) and *SAS*-basis (right column) in Fig. 5b. For the *SAS*-basis 331 state the overlap is very small for all values of Δ_{SAS} , $\Delta\rho$ or layer separation d . On the other hand, the overlap with the layer-basis 331 state is non-zero for moderate values of Δ_{SAS} and for $1 \leq d \leq 4$ the overlap is large and, despite the fact that non-zero $\Delta\rho$ eventually destroys the 331, it is remarkably robust to charge imbalancing.

In Figs. 6 and 7 we show a clearer view of the overlaps. In particular, for $d = 0$ when the system is $SU(2)$ symmetric it is obvious in Figs. 6 and 7 that the layer-basis and *SAS*-basis are merely pseudo-spin rotations of one another. Furthermore, it is clear that for $d = 0$ there is no region in phase-space where the Halperin 331 wavefunction (in either basis) is a good description and only upon increasing d away from zero do we see any sort of reasonably sized overlaps when increasing Δ_{SAS} (though it should be noted that for $d = 1$ and 2 the overlap with 331

is sizable for small values of both Δ_{SAS} and $\Delta\rho$). For the half-filled Landau level at $d = 0$, theoretically, the system is known to be spin-polarized^{42,43}, or one-component, so it is not surprising that a two-component wavefunction like the Halperin 331 state would not be a good description and, therefore, have a small overlap with the exact ground state. Note also that the one-component Moore-Read Pfaffian is also not a good description for the $d = 0$ case since, in the lowest Landau level, the ground state is most likely a non-FQHE (Composite Fermion) Fermi sea^{18,80}.

Generally, on the example of our $N = 8$ system we can conclude that (i) when the system is largely two-component in nature then the overlap between the exact ground state and the Halperin 331 state is large, and (ii) when the system is largely one-component in nature the overlap between the exact ground state and the Pf is large. This is more clearly shown in Fig. 5c where in the left and right columns we show the expectation value of $(N_R - N_L)/2$ and $(N_S - N_{AS})/2$, respectively. When the system is largely one-component, either in the layer sense or *SAS* sense, the system concomitantly has a sizable overlap with the one-component Pf state and when the system is largely two-component the overlap with the Halperin 331 state is large. Again, Fig. 8 shows the pseudo-spin expectation values clearer for a few specific examples of layer separation d —note again how non-zero d destroys the symmetry between the layer- and *SAS*-basis obtained when $d = 0$ and the system is $SU(2)$ symmetric. We emphasize that the first conclusion (i) is not affected by finite-size effects, whereas the conclusion (ii) likely holds only for a few special systems such as $N = 8$ and it may be a finite-size artifact.

In Fig. 10 we show a schematic diagram that encapsulates broad features of the bilayer model (and WQW model) for small layer separation d (small WQW width W). For large Δ_{SAS} and small $\Delta\rho$ the system is one-component in the *SAS*-basis and for large $\Delta\rho$ and small Δ_{SAS} the system is one-component in the layer-basis. When, both tunneling strengths approach zero, the system is two-component in the layer-basis, the *SAS*-basis, or both. The diagram would be topologically similar for non-zero (and even large) values of layer separation d and WQW width W . The only difference is that the diagram would not be symmetric between Δ_{SAS} and $\Delta\rho$ since the system is not $SU(2)$ symmetric.

Lastly, in Fig. 5d we show the FQHE energy gap. For $d \lesssim 1$ the FQHE energy gap is relatively constant as Δ_{SAS} and $\Delta\rho$ vary. When d is increased past approximately $d \sim 2$ the FQHE gap shows interesting features as a function of the strength of the two tunneling terms. Somewhat surprisingly, the FQHE gap obtains a maximum for non-zero Δ_{SAS} and finite d (this is related to similar results found recently in Ref. 5 where the FQHE gap is maximum on the “ridge” as a function of Δ_{SAS} and separation d for zero charge imbalance $\Delta\rho$). This “ridge” basically separates the regions in the quantum phase diagram where the system is either in the Pf or

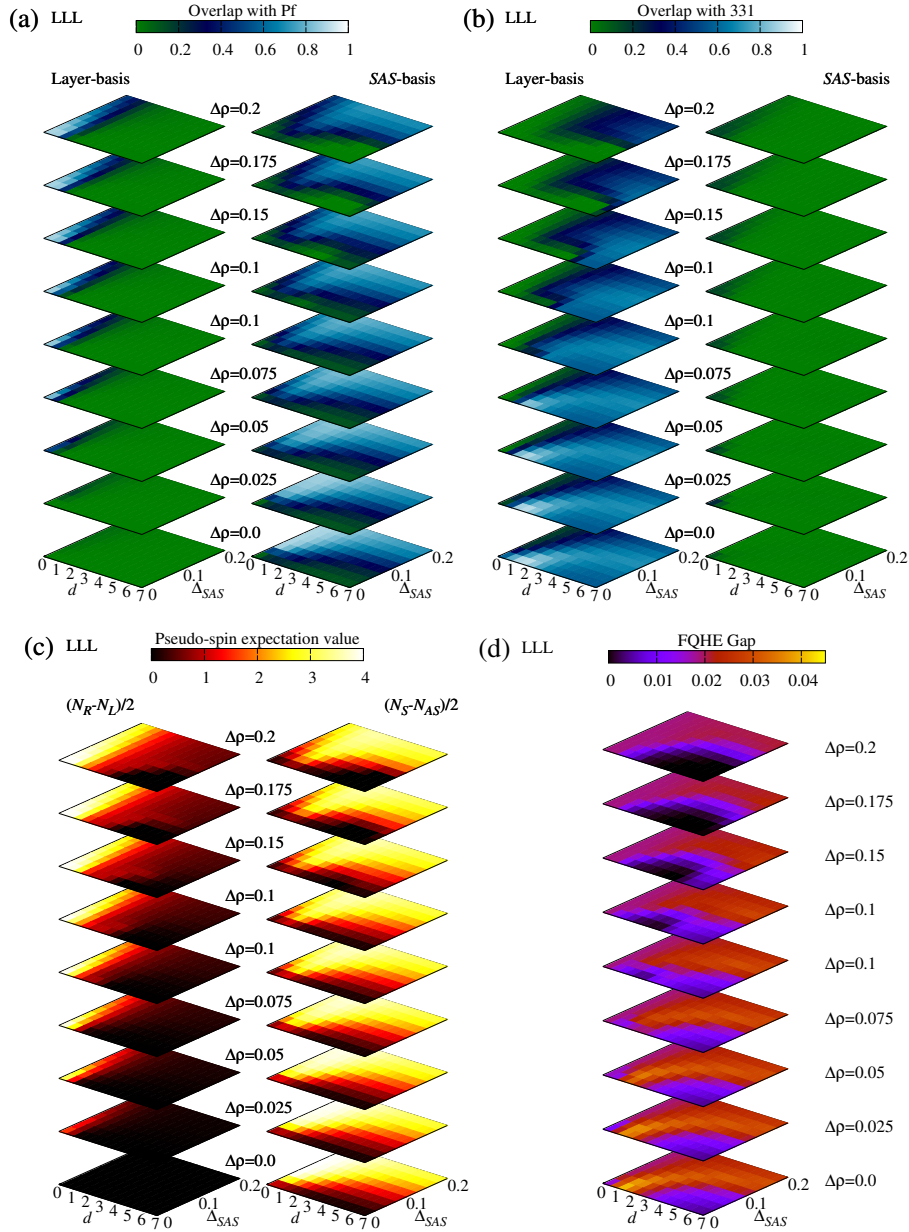


FIG. 11. (Color online) Lowest Landau level: Same as Fig. 5 except that all plots are shown as a function of inter-layer tunneling Δ_{SAS} and layer separation d for a number of different charge imbalances $\Delta\rho$ and zero individual layer thickness $w = 0$.

331 phase. Fig. 9 is a more detailed depiction of the FQHE energy gap.

Before moving on to results for the second Landau level we show essentially the same results as Fig. 5a-d but as a function of Δ_{SAS} and layer separation d for several values of $\Delta\rho$ in Fig. 11a-d. This presentation is to more easily compare with previous bilayer works^{4,5} where the data was presented this way. When considering the overlap between the exact ground state and the Pf we see that increasing imbalance (increasing $\Delta\rho$) eventually produces a high overlap for small values of d in the layer-basis. In the *SAS*-basis, charge imbalance pushes the maxi-

um overlap to larger values of Δ_{SAS} and slightly larger values of d while generally decreasing the overlap along the way. For the overlap with the Halperin 331 wavefunction it is clear that there is no region in parameter space that produces a sizable overlap in the *SAS*-basis. For the layer-basis 331, the overlap is large for moderate layer separation ($d \sim 1 - 2$) and Δ_{SAS} . The position of the maximum overlap is relatively constant as a function of $\Delta\rho$ until $\Delta\rho \sim 0.1$ when the maximum overlap shifts to higher values of d and decreases markedly in magnitude. The expectation values of the pseudo-spin operators (Fig. 11c) mirrors the results of the overlap

calculations.

For the FQHE gap shown in Fig. 11d we see the familiar picture found in Ref. 5. We first reiterate that result. For $\Delta\rho = 0$, the FQHE gap is largest along a “ridge” in Δ_{SAS} - d space and the overlap between the SAS -basis Halperin 331 state is largest in the region of phase space where the system is two-component and the overlap between the SAS -basis Pf state is largest in the region of phase space where the system is largely one-component. The FQHE gap “ridge” seems to function as the phase boundary between the two states in the quantum phase diagram, however, the maximum FQHE gap is slightly on the Halperin 331 side of the phase diagram and the experimentally observed^{62–65} FQHE at $\nu = 1/2$ is of that nature. This is strongly thought to be the case because of recent work by Storni *et al.*⁵⁸ that showed that in the lowest Landau level the FQHE gap for one-component systems vanishes in the thermodynamic limit—even though it is non-zero in our finite size calculation. Thus, our non-zero gap in the Pf region of the phase diagram for the lowest Landau level is most likely a finite size effect.

For non-zero $\Delta\rho$ the above picture changes. The “ridge” is weakened and a maximum in the FQHE gap starts to appear for large Δ_{SAS} and large d until eventually weakening further. In the large $\Delta\rho$ limit we see a SAS -basis Pf state for large Δ_{SAS} and non-zero d and a layer-basis Pf for moderate Δ_{SAS} and very small d . However, we caution that the FQHE gap is globally weakened upon inclusion of $\Delta\rho$ and taking into account recent results⁵⁸, an experimental system would most likely not exhibit the FQHE in that region of parameter space.

To summarize our results from the calculations on the sphere in the lowest Landau level, we find a robust layer-basis 331 state that has high overlap with the exact ground state and dominant gap in the phase diagram. Furthermore, we find a one-component state that has some properties of the Moore-Read Pfaffian, but it is likely to show up as a compressible state in experiments. These conclusions are in agreement with the results of Ref. 83 (and consistent with Ref. 58) where transitions between 331 state, Pfaffian and Composite Fermion Fermi sea were studied in a bilayer model with tunneling Δ_{SAS} (in the layer-basis) using exact diagonalization and effective mean field BCS theory of Read-Green⁵⁰. There it was found that the increase of inter-layer tunneling converts the 331 state into a Composite Fermion Fermi sea because the effective chemical potential of “even”-channel electrons becomes very large. Similar analysis is expected to apply when $\Delta\rho$ is large and the system is viewed in SAS -basis.

B. Wide-quantum-well

We now turn to the wide-quantum-well (WQW) model which largely mirrors the results presented for the bilayer model. However, there are some differences between the two models which we point out below.

Fig. 12 shows the overlap between the Moore-Read Pfaffian wavefunction (in both the SAS -basis and the layer-basis) and the exact ground state of the WQW model as a function of Δ_{SAS} and $\Delta\rho$ for a few values of the WQW width W . This figure should be compared with Fig. 6 for the bilayer model. *Qualitatively*, the two models produce very similar results. Of course, a layer separation of d in the bilayer model is not equivalent to the WQW width W and any similarities between the two at $d \sim W$ is coincidental. However, the behavior for the bilayer model as d increases is the same as the behavior for the WQW model as W increases. That is, for small $W = 0.4$, the overlap between the exact ground state and the one-component Pf in the layer-basis becomes large when $\Delta\rho$ is increased since the system is being driven to be more one-component in the layer sense. When Δ_{SAS} is increased, the overlap between the exact ground state and the Pf in the SAS -basis becomes large since the system is being driven to be one-component in the SAS -basis.

Note, however, that for $W = 0.4$ (Fig. 12a) the system is not as symmetric upon $\Delta_{SAS} \leftrightarrow \Delta\rho$ as it was for the $d = 0$ bilayer model case where the model was actually $SU(2)$ symmetric. This is because the WQW model is not $SU(2)$ symmetric for small W because even as W becomes very small the Coulomb energy between electrons in the S and AS states is never equal, i.e., the AS state always has a node and therefore higher kinetic energy. That being said, the models produce very similar results.

In Fig. 13 we show the overlap between the exact ground state of the WQW model and the Halperin 331 state. This time, as opposed to Fig. 7 we only show the overlap with the 331 state written in the layer-basis since, as we learned previously by studying the bilayer model results, and by confirming this with the WQW model, the overlap between the ground state of the WQW model and the SAS -basis 331 state is always nearly zero, hence, we do not bother to show these results explicitly. For the layer-basis 331, however, we again see qualitatively similar behavior compared to the bilayer model. For small W the overlap with the 331 state is very small and it can be increased by increasing W . One interesting difference between the results of the two models is that for $W = 5$ the maximum overlap with 331 has a maximum for non-zero Δ_{SAS} for the WQW model. Furthermore, non-zero charge imbalance $\Delta\rho$ eventually destroys the Halperin 331 state by driving the system to be one-component, however, the 331 state is remarkably robust to charge imbalancing.

Similar to the bilayer model, the pseudo-spin expectation value for the WQW model in Fig. 14 mirrors the behavior of the overlaps. When the system is largely one-component, either in the layer- or SAS -basis (large value of $(N_R - N_L)/2$ or $(N_S - N_{AS})/2$, respectively), the overlap with the appropriate basis Pf state is large. When the system is two-component the overlap with the 331 is large. In investigating the pseudo-spin expecta-

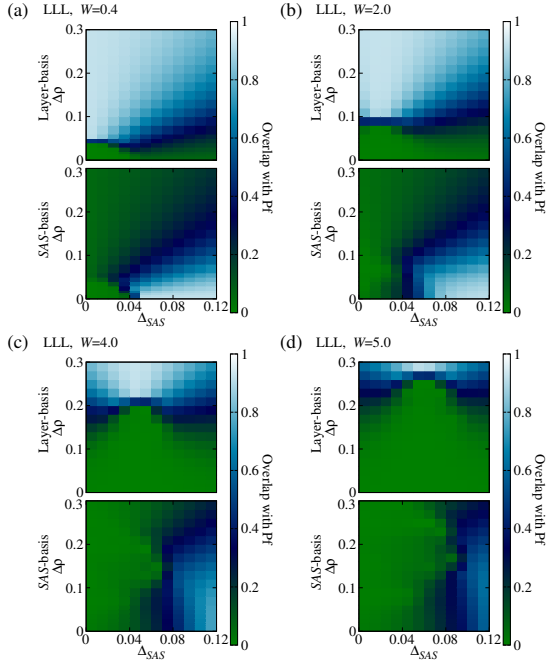


FIG. 12. (Color online) Lowest Landau level: Wavefunction overlap between the Moore-Read Pfaffian wavefunction in the layer-basis (top panel) and the SAS -basis (lower panel) and the exact ground state for the WQW for (a) $W = 0.4$, (b) $W = 2$, (c) $W = 4$ and (d) $W = 5$.

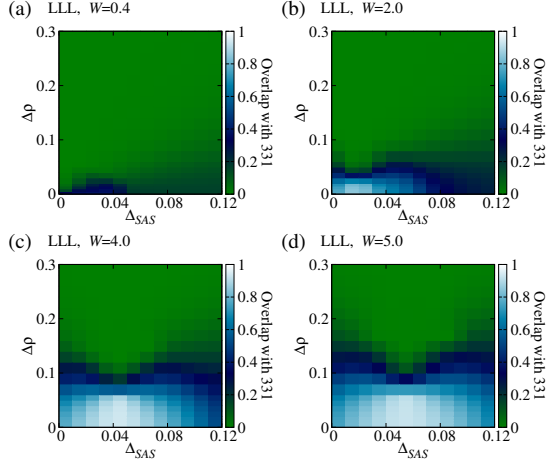


FIG. 13. (Color online) Lowest Landau level: Wavefunction overlap between the Halperin 331 wavefunction in the layer-basis and the exact ground state for the WQW for (a) $W = 0.4$, (b) $W = 2$, (c) $W = 4$ and (d) $W = 5$.

tion value for the WQW model we see the most serious discrepancy between the two models—this effect was also seen previously in Ref. 4. For $W \geq 2$, and relatively small values of Δ_{SAS} , the ground has a negative value of $(N_S - N_{AS})/2$. This means that the electrons occupy the AS state compared to the S state. If we recall the overlap between the exact ground state and the Moore-Read Pfaffian in the SAS -basis (lower panel of Fig. 12)

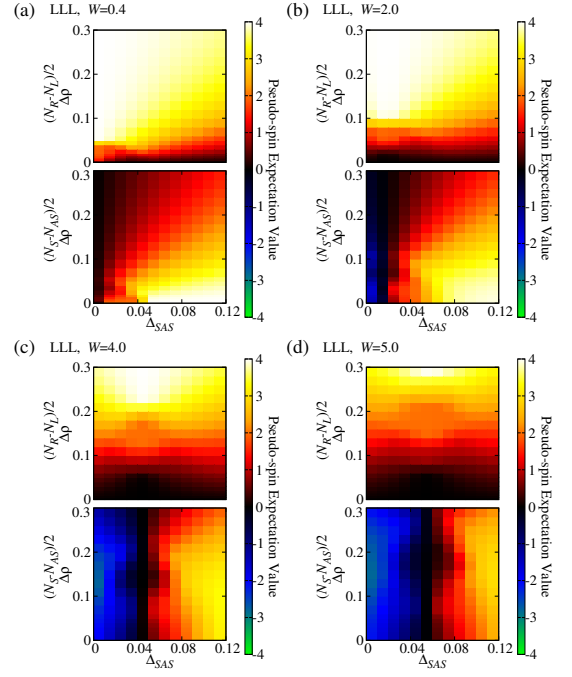


FIG. 14. (Color online) Lowest Landau level: (Pseudo-spin) expectation value of the exact ground state (for the WQW model) of $(N_R - N_L)/2$ (top panel) and $(N_S - N_{AS})/2$ (lower panel) for (a) $W = 0.4$, (b) $W = 2$, (c) $W = 4$ and (d) $W = 5$. Note that the WQW model always breaks $SU(2)$ symmetry even for small W .

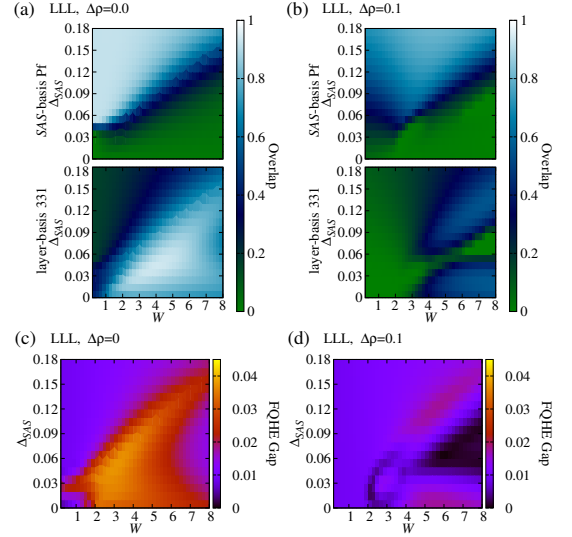


FIG. 15. (Color online) Lowest Landau level: FQHE energy gap for the WQW model as a function of W and Δ_{SAS} with (c) $\Delta\rho = 0$ (left column) and (d) $\Delta\rho = 0.1$ (right column). Also shown is the overlap between the SAS -basis Moore-Read Pfaffian (top panel) and the layer-basis Halperin 331 (bottom panel) wavefunctions and the exact ground state for (a) $\Delta\rho = 0$ and (b) $\Delta\rho = 0.1$.

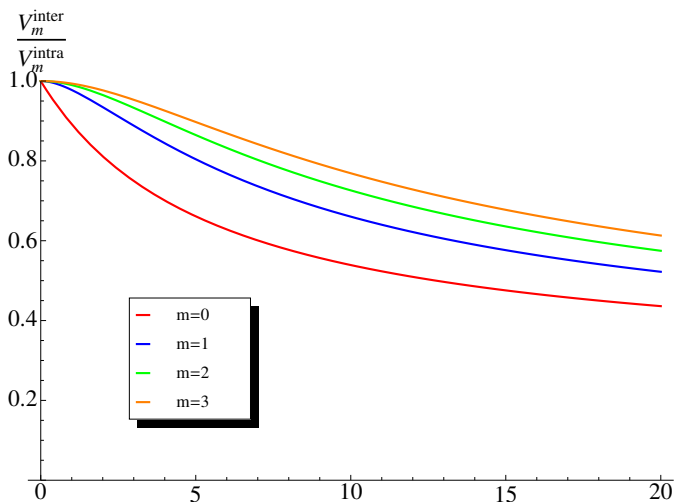


FIG. 16. (Color online) Ratio of the few strongest, inter-layer and intra-layer (bilayer) pseudopotentials $V_m^{\text{inter}}/V_m^{\text{intra}}$ derived using the WQW model⁴ as a function of width W . Note the saturation of the ratios for large widths W , illustrating the limit of validity of the WQW to describe bilayers.

the overlap is large for large Δ_{SAS} and this behavior mirrors the large value of $(N_S - N_{AS})/2$ shown in the lower panel of Fig. 14. However, the one-component Moore-Read Pfaffian we consider pairs electrons in the S state (shown schematically in Fig. 4b). We have not checked the overlap with the one-component Pf written such that the pairing occurs between electrons in the AS state, thus, adding another version of the Pf. By examining the value of $(N_S - N_{AS})/2$ for $W \geq 2$ in the small Δ_{SAS} region of phase space we would expect a reasonable value of the overlap with a one-component Pf pairing electrons in the AS state.

The WQW model is more general than the usual bilayer model and the latter can be derived from it (see Section IV-B of Ref. 4 for a detailed discussion). However, if the well width W becomes very large, it is unjustified to restrict the model to only the lowest two subbands (and the inclusion of higher subbands cannot be treated exactly because of the computational complexity). On the other hand, as we map the WQW Hamiltonian to an effective bilayer, we find that the effective bilayer distance \tilde{d} saturates for large W . To see this, we can calculate the Haldane pseudopotentials $V_m^{\sigma_1\sigma_2\sigma_3\sigma_4}$, where m is the relative angular momentum of the two electrons and $\sigma = S, AS$. If we denote by $\mathcal{F}^{\sigma_1\sigma_2\sigma_3\sigma_4}(\mathbf{r})$ the effective interaction in the plane, we have

$$\mathcal{F}_{\sigma_1\sigma_2\sigma_3\sigma_4}(\mathbf{r}) = \int_0^W dz_1 \int_0^W dz_2 \langle \mathbf{r} | \sigma_1 \rangle (z_1) \langle \mathbf{r} | \sigma_2 \rangle (z_2) \frac{1}{\sqrt{r^2 + |z_1 - z_2|^2}} \langle \mathbf{r} | \sigma_3 \rangle (z_1) \langle \mathbf{r} | \sigma_4 \rangle (z_2). \quad (8)$$

The Haldane pseudopotentials for the effective interaction, written on the disk for simplicity (for the lowest

Landau level), are

$$V_m^{\sigma_1\sigma_2\sigma_3\sigma_4} = \int \frac{d^2\mathbf{k}}{(2\pi)^2} e^{-k^2} \mathcal{L}_m(k^2) \mathcal{F}_{\mathbf{k}}^{\sigma_1\sigma_2\sigma_3\sigma_4},$$

where \mathcal{L}_m is the Laguerre polynomial and the Fourier transform $\mathcal{F}_{\mathbf{k}}^{\sigma_1\sigma_2\sigma_3\sigma_4}$ can be evaluated analytically. Furthermore, we can construct linear combinations⁴ of $V_m^{\sigma_1\sigma_2\sigma_3\sigma_4}$ to get the effective bilayer pseudopotentials, V_m^{intra} and V_m^{inter} . We plot the ratios of the few strongest V_m^{intra} and V_m^{inter} in Fig. 16 as a function of W . Notice that the limits saturate for large W , indicating that the inter-layer repulsion decreases very slowly with respect to intra-repulsion for larger W , thus suggesting that the model becomes unrealistic in this regime. Also that the pseudopotentials involving a node in the z -wave function (the AS single particle wavefunction has one node) can be smaller in absolute value than those without a node, indicating a possibility for some W to have a depopulation of the lowest subband and negative polarization ($N_S - N_{AS}$), as seen in the data.

Fig. 15 shows the FQHE energy gap for the WQW model for $\Delta\rho = 0$ and $\Delta\rho = 0.1$, respectively. For $\Delta\rho = 0$, we see similar behavior to the results of the bilayer model and shown previously⁵, i.e., Fig. 11d for $\Delta\rho = 0$. Of course, there are quantitative differences between the two models but the FQHE energy gap still shows a prominent “ridge” as a function of Δ_{SAS} and W . The ridge marks the transition line between the 331 and the Pfaffian, or perhaps compressible states. Also, note that the maximum FQHE gap (the “ridge”) is slightly on the Halperin 331 side of the quantum phase diagram if the phase boundary is taken to be the place at which the 331 overlap is larger than the Pfaffian overlap, i.e., the 331 phase is the region where the Halperin 331 overlap is larger than the Pfaffian and vice versa. cf. Figs. 15a and b. When the charge imbalancing term is increased to $\Delta\rho = 0.1$ the FQHE gap is markedly reduced, as it was in the bilayer model. Again, as for $\Delta\rho = 0$ the maximum gap is in the Halperin 331 part of the phase diagram. Interestingly, there appear to be two “ridges” forming for the $\Delta\rho = 0.1$ situation in the FQHE gap and both “ridge” maxima are mirrored peaks in the 331 overlap—although, note that the overlaps (both 331 and Pf) for the $\Delta\rho = 0.1$ situation are never very large and in a real experimental system the phase would most likely have been taken over by some other competing phase by the time the charge imbalancing strength reaches $\Delta\rho = 0.1$, namely a striped phase or, perhaps, a (Composite Fermion) Fermi sea.

1. Torus geometry

In this section we consider the wide-quantum-well model in the torus geometry^{84–86} which has one distinct advantage to the spherical geometry (of course, at the cost of other disadvantages). Recall in the spherical geometry, the filling factor is defined as $\lim_{N \rightarrow \infty} N/N_\phi$ and

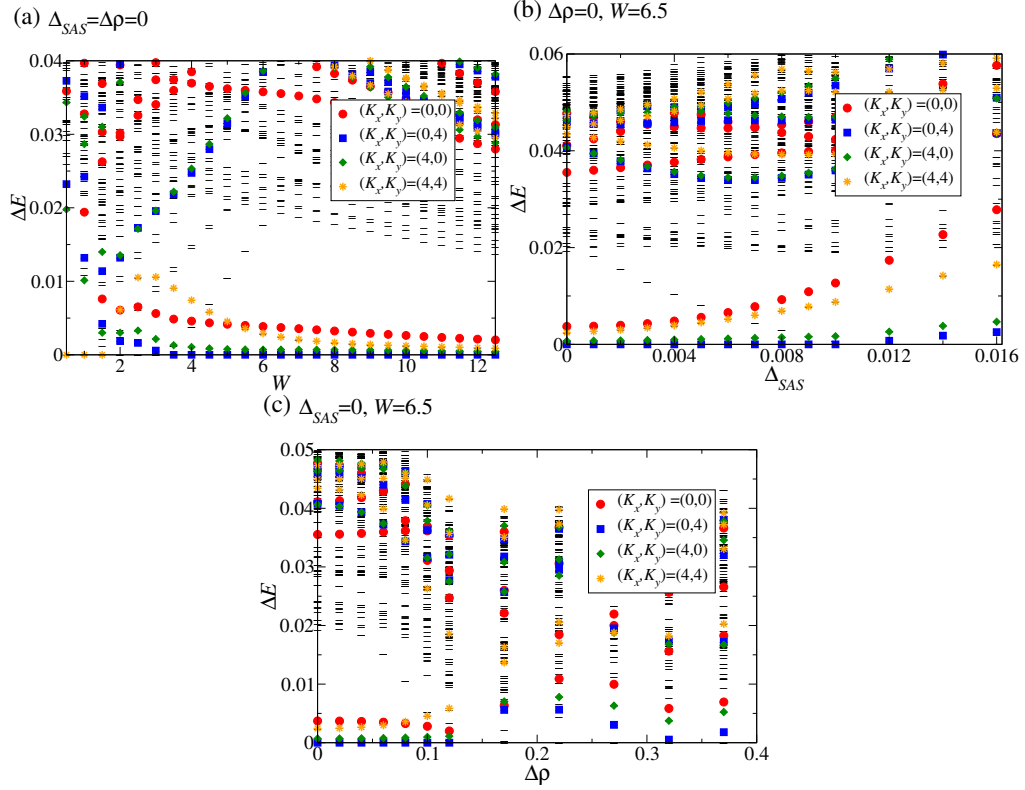


FIG. 17. (Color online) Lowest Landau level: Energy spectra (given as the energy ΔE with respect to the ground state) for different pseudo-momenta (the different levels) with (a) $\Delta_{SAS} = \Delta\rho = 0$ as a function of WQW width W , (b) $W = 6.5$ and $\Delta\rho = 0$ as a function of Δ_{SAS} and (c) $W = 6.5$ and $\Delta_{SAS} = 0$ when the imbalance $\Delta\rho$ is increased from zero. The pseudo-momenta corresponding to the Halperin 331 state and Moore-Read Pfaffian state $((K_x, K_y) = (0, 0)$ (solid red circle), $(0, 4)$ (solid blue square), $(4, 0)$ (solid green diamond) and $(4, 4)$ (orange star) and $(K_x, K_y) = (0, 4)$, $(4, 0)$ and $(4, 4)$, respectively. The black dashes correspond to states with pseudo-momenta not belonging to either the 331 or Pf states.

the relationship between N and N_ϕ for the Moore-Read Pfaffian and Halperin 331 is $N_\phi = 2N - 3$ where the “-3” is a consequence of the curvature of a spherical surface. Other competing phases for a half-filled Landau level, such as a (Composite Fermion) Fermi sea, have a different shift and comparing different states on an equal footing requires great care and extrapolation to the thermodynamic limit. However, on the torus, the filling factor is uniquely defined as simply N/N_ϕ and, therefore, different states can be directly compared for finite size systems—of course, this does not mean a conclusion made for a finite sized system will maintain as the thermodynamic limit is approached. (We note that it makes no sense to consider overlaps extrapolated to the thermodynamic limit since they trivially vanish.)

The torus geometry is generally defined using a domain with sides of length a and b with $a \neq b$. The aspect ratio of the toroidal system is $\tau = a/b$. The magnetic field does not allow the use of the usual translation operators but many-body states can be found⁸⁶ using the so-called magnetic translation operators with conserved pseudo-momenta (K_x, K_y) . The pseudo-momenta belong to a Brillouin zone with $(K_x = 2\pi s/a, K_y = 2\pi t/b)$ with

$s, t = 0, \dots, N_0 - 1$ with N_0 being the greatest common divisor of N and N_ϕ .

Different FQHE states on the torus can be specified by their ground state (topological) degeneracy. Generically, for a Landau level filling factor of p/q there is always a center-of-mass degeneracy equal to q which is invariant to the form of the Hamiltonian and, thus, of no physical significance—we shall ignore it. Also there can be additional degeneracies that occur at special points in the Brillouin zone, such as at certain points in a hexagonal Brillouin zone, and we will consider these trivial. Finally, there can be degeneracies that are related to the specific topological nature of certain ground states and, therefore, non-trivial. For the two-component (Abelian) Halperin 331 state⁸⁷ we expect a quadruplet of states (up to the center of mass degeneracy, which in our case is 2) one of which belongs in the $(K_x, K_y) = (0, 0)$ sector and the remaining three are at the Brillouin zone corners $(K_x, K_y) = (0, N_0/2)$, $(N_0/2, 0)$, and $(N_0/2, N_0/2)$. The non-Abelian Moore-Read Pfaffian^{46,88} has only a *three-fold* degeneracy⁵⁰ of $(K_x, K_y) = (0, N_0/2)$, $(N_0/2, 0)$, and $(N_0/2, N_0/2)$, i.e., the $(K_x, K_y) = (0, 0)$ state is missing. Compressible states, such as the (Composite

Fermion) Fermi sea, generally do not have clearly defined degeneracies—they may have accidental degeneracies that are strong functions of the aspect ratio τ , particle number N , or other Hamiltonian parameters. The *exact* degeneracies are expectations based on the (analytic) form of the variational ansatz wavefunctions and their respective conformal field theories^{46,79}. The ground state(s) of an actual Hamiltonian will not display exact degeneracies^{39,59,60,80} (perhaps they do in the thermodynamic limit?) but the ground state(s) should qualitatively show the ground state topological degeneracy corresponding to the variational ansatz if they are to be thought of as being in that “phase”. Many states are sensitive to changes in τ while others are not. One should really investigate the properties of the system with regard to changes in τ , however, in the present case, a somewhat involved analytical calculation regarding the “background” charge is needed, and so we focus here on a fixed aspect ratio of $\tau = 0.97$.

All results on the torus correspond to a system of $N = 8$ electrons in the half-filled lowest Landau level— $\nu = 1/2$. Fig. 17a shows the energy spectrum of the low-lying states for the WQW model in the absence of any tunneling terms, i.e., $\Delta_{SAS} = \Delta\rho = 0$, as a function of the WQW width W . For each W , the lowest-lying energies are plotted relative to the ground state and shape- and color-coded to emphasize which states belong to which pseudo-momenta sectors expected when considering the two-component Halperin 331 and one-component Moore-Read Pfaffian wavefunctions. Namely, we track the pseudo-momenta sectors $(K_x, K_y) = (0, 4)$, $(4, 0)$ and $(4, 4)$ for the Pf with the addition of $(K_x, K_y) = (0, 0)$ for the 331 state. For large widths $W > 4.5$, the spectrum is characterized by a large energy gap separating a high-energy (quasi-)continuum of states from a low-energy, nearly degenerate manifold of states at the pseudo-momenta corresponding to the 331 state. As the width is decreased towards zero the $(K_x, K_y) = (0, 0)$ state that specifies the Halperin 331 state from the Moore-Read Pfaffian state goes up in energy joining the continuum. However, the $(K_x, K_y) = (0, 4)$ and $(4, 0)$ states of the Moore-Read Pfaffian also rise in energy into the continuum while at the same time a few states from the continuum drop down in energy mixing with states belonging to the 331 or Pf states. Finally, at very small $W < 1$ there is a single ground state of $(K_x, K_y) = (4, 4)$ and a large energy gap. However, there is no three-fold degeneracy characteristic of the Moore-Read Pfaffian state present.

In Fig. 17b we fix $W = 6.5$ and $\Delta\rho = 0$ and vary the inter-layer tunneling strength Δ_{SAS} . For small $\Delta_{SAS} = 0$ we are clearly in the Halperin 331 part of the phase diagram since the spectra has a quasi-four-fold degeneracy characteristic of the 331 phase separated from the continuum by a large energy gap. Upon increasing Δ_{SAS} in an attempt to drive the system into the Moore-Read Pfaffian phase we see that while the $(K_x, K_y) = (0, 0)$ state of the 331 phase rise in energy and joins the continuum, the

$(K_x, K_y) = (4, 4)$ state of the Pfaffian phase goes with it and a state from the high-energy continuum drops down into a quasi-three-fold degeneracy. However, this quasi-three-fold degeneracy does not contain the right pseudo-momenta to describe the non-Abelian Moore-Read Pfaffian phase.

Lastly, in Fig. 17c we again set $W = 6.5$ but now fix $\Delta_{SAS} = 0$ and vary the charge imbalance $\Delta\rho$. As before, for small $\Delta\rho$ we see a clear signature of the Halperin 331 phase. However, as $\Delta\rho$ is increased the energy gap essentially collapses giving way to a phase that would most likely not exhibit the FQHE.

These conclusions corroborate our previous work using the spherical geometry and agree with the previous study⁸³ of bilayer model on the torus for $\nu = 1/2$. Namely, the Halperin 331 state is a good ansatz for the FQHE in the right parameter regions for bilayer and WQW systems. However, when the system is driven to be one-component in the hopes of producing a FQHE described by the Moore-Read Pfaffian state the Hamiltonian details and Haldane pseudopotential⁸¹ values are such that the Moore-Read Pfaffian phase loses out to a different, most likely, non-FQHE state such as a striped phase or (Composite Fermion) Fermi sea.

V. RESULTS: SECOND LANDAU LEVEL

In this section we present results of our calculations for the second Landau level, that is, bilayer FQHE at $\nu = 5/2$. (Work⁸⁹ has been done considering bilayer FQHE where the total filling factor is $\nu = 5/2 + 5/2 = 5$ but it is unrelated to our work.) We are neglecting Landau level mixing and considering the electrons occupying the second Landau level to be spin-polarized. Operationally, we have projected the half-filled electrons in the second Landau level into the lowest Landau level using the Haldane pseudopotentials⁸¹. These effective pseudopotentials take into account the screening of the Coulomb interaction that occurs between the electrons in the SLL due to the (taken to be) inert electrons in the LLL. We will not detail the procedure of using Haldane pseudopotentials in the FQHE as this procedure has been given in many places^{12,81}. Also, we (Peterson and Das Sarma⁵) have recently studied the FQHE in the SLL *without* the presence of a charge imbalancing term and will compare our results here extensively with the ones given previously.

Before we tackle the results for the second Landau level we briefly note that bilayer systems in higher Landau levels are quite subtle and non-trivial and actually provide some conceptual difficulty. As recently discussed in Ref. 5, it is not obvious what happens to the electrons in the lowest spin-up and spin-down Landau levels when driving a one-component system at $\nu = 5/2$ to a two-component (bilayer) system at total filling $\nu = 5/2$. For this work, however, we take the conceptually well-defined and straightforward solution⁵: we assume full

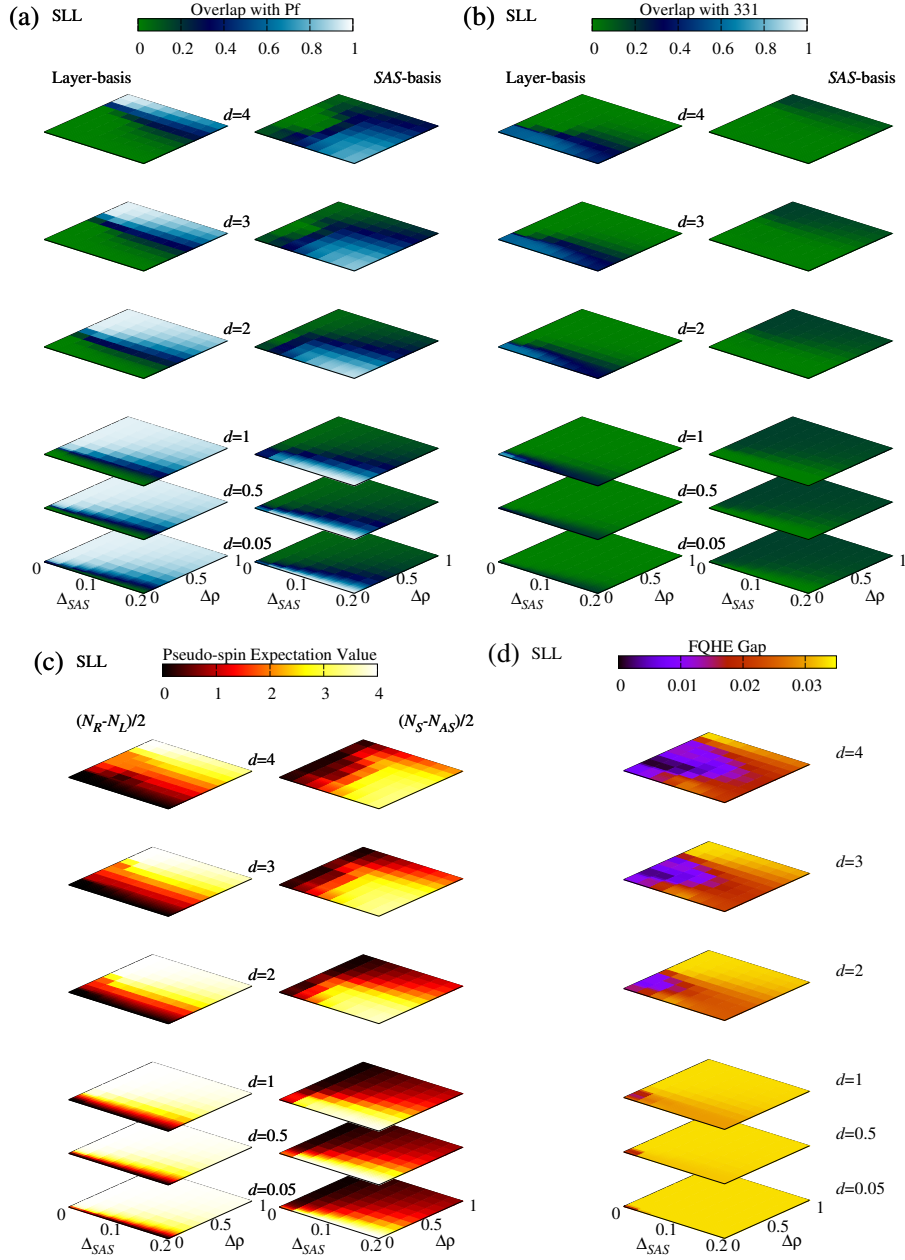


FIG. 18. (Color online) Second Landau level: (a) Wavefunction overlap between the exact ground state of the bilayer Hamiltonian and the Moore-Read Pfaffian written in the layer-basis (left column) and the SAS-basis (right column) shown as a function of inter-layer tunneling Δ_{SAS} and charge imbalance $\Delta\rho$ for different values of layer separation d and zero individual layer thickness $w = 0$. (b) Same as (a) but for the Halperin 331 wavefunction. (c) Pseudo-spin expectation value or, more physically, the expectation value of $(N_R - N_L)/2$ (left column) and $(N_S - N_{AS})/2$ (right column) as a function of Δ_{SAS} and $\Delta\rho$. (d) The FQHE energy gap for the exact bilayer Hamiltonian.

spin-polarization, hence the system is essentially spinless with each Landau level having only one spin-index. Then the $\nu = 5/2$ (balanced) two-component system is equivalent to one where each layer has $1 + 1/4$ filling with the lowest spin Landau level being completely full and the second Landau level being $1/4$ full. In this way, the incompressible FQHE states (Halperin 331 or Moore-Read Pfaffian) form completely in the second Landau

level. This “solution” provides a completely well-defined mathematical problem. Of course, the real physical system, i.e., bilayer FQHE systems in higher Landau levels, could be more complicated and produce rich physics. In fact, theoretically, the *full* solution is out of reach for any conceivable computer—the Hilbert space is too vast when including many (or at least three) Landau levels, spin-up and spin-down, and layer index. Thus, theoretical and

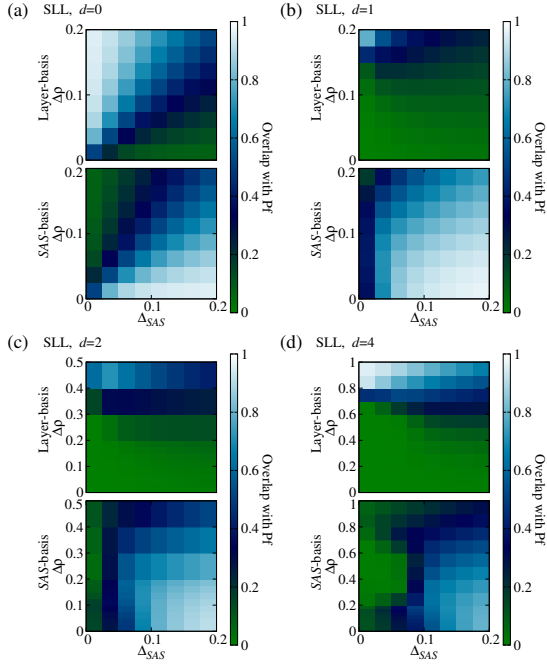


FIG. 19. (Color online) Second Landau level: Wavefunction overlap between the Moore-Read Pfaffian wavefunction in the layer-basis (top panel) and the SAS -basis (lower panel) and the exact ground state for (a) $d = 0$, (b) $d = 1$, (c) $d = 2$ and (d) $d = 4$.

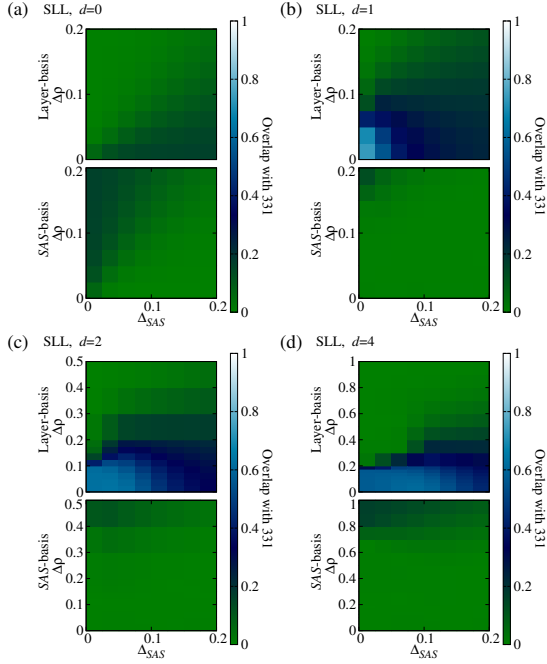


FIG. 20. (Color online) Second Landau level: Wavefunction overlap between the Halperin 331 wavefunction in the layer-basis (top panel) and the SAS -basis (lower panel) and the exact ground state for (a) $d = 0$, (b) $d = 1$, (c) $d = 2$ and (d) $d = 4$.

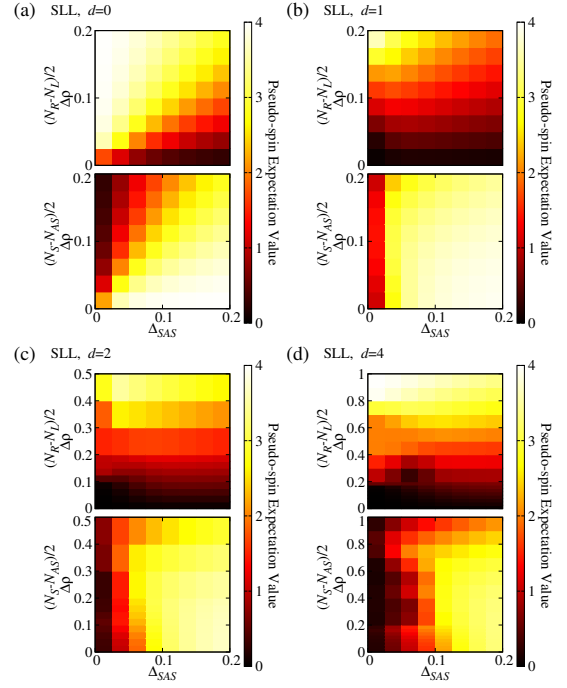


FIG. 21. (Color online) Second Landau level: (Pseudo-spin) expectation value of the exact ground state of $(N_R - N_L)/2$ (top panel) and $(N_S - N_{AS})/2$ (lower panel) for (a) $d = 0$, (b) $d = 1$, (c) $d = 2$ and (d) $d = 4$.

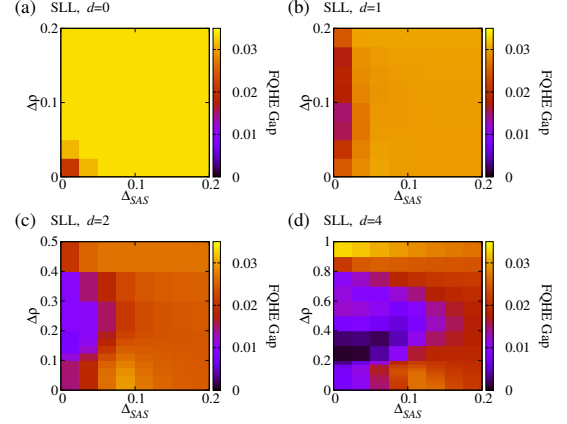


FIG. 22. (Color online) Second Landau level: FQHE energy gap for (a) $d = 0$, (b) $d = 1$, (c) $d = 2$ and (d) $d = 4$.

experimental efforts in studying bilayer FQHE systems in higher Landau levels is likely a fertile ground for new discoveries.

A. Bilayer

In Fig. 18 we show overlaps between the exact ground state and the layer-basis and SAS -basis Pf and 331 wavefunctions, pseudo-spin expectation values, and the FQHE gap for the second Landau level. The difference between the LLL and the SLL are subtle but important.

First we focus on the overlaps between the Pf and 331 states and the exact ground state in both the layer- and *SAS*-bases, cf. Fig. 18a-b. The main difference between the results in the LLL and the SLL is that, as has been shown previously^{5,59,60} for the case of zero charge imbalance $\Delta\rho = 0$, the overlap between the exact state and the Pf state(s) is higher in the SLL than it is in the LLL. In the SLL, the Pfaffian overlap is approximately ~ 0.97 at its largest while in the LLL it is approximately ~ 0.9 at its largest. This can be seen more clearly in Fig. 19 where, compared to the results of the LLL, the overlap with the Pf state is higher in the SLL. (Again, for $d = 0$ the system is $SU(2)$ symmetric and the layer-basis and *SAS*-basis results are related via a pseudo-spin rotation.) We note that by increasing the width of the individual quantum well w , the Moore-Read Pfaffian overlap can be increased to nearly unity^{5,59,60}. This is a consequence of the differences between the Haldane pseudopotentials corresponding to the LLL versus those of the SLL with the SLL pseudopotentials being more amenable to pairing into a p -wave paired BCS state (of Composite Fermions), i.e., the Moore-Read Pfaffian^{42,56,59,60,80,90}.

There is another striking difference between the results in the LLL versus the SLL when considering the overlap between the Halperin 331 state. In the LLL, the 331 state provides a very good description of the FQHE for two-component systems when the separation d (or wide-well width W for the wide-quantum-well) and the tunneling strengths are appropriate—this is evident by the value high value of the overlap that is obtained (~ 0.99). In the SLL, the qualitative behavior of the overlap as the system parameters are varied is similar to the LLL but the overlap does not obtain as high a value (only ~ 0.8 for $d \sim 1$ and $\Delta_{SAS} = \Delta\rho = 0$). This, again, can be seen more clearly in Fig. 20.

Looking at the pseudo-spin expectation value $\langle \hat{S}_z \rangle = (N_S - N_{AS})/2$ and $\langle \hat{S}_z \rangle = (N_R - N_L)/2$ in Fig. 18c (as well as Fig. 21) we see very little difference between the lowest and second Landau levels. In fact, visually it is difficult distinguishing the two.

Lastly, we consider the FQHE gap (Fig. 18d and Fig. 22), which does display some behavior that is qualitatively different from that of the LLL. This qualitatively different behavior manifests itself for values of layer separation $d > 2$. In this region of parameter space we see that for increasing values of $\Delta\rho$ the FQHE gap has a maximum for a wide range of Δ_{SAS} . This is in stark contrast to the FQHE gap in the LLL (cf. Fig. 5d) where the gap shows some indication of increasing for increasing $\Delta\rho$ but not to a *maximum*.

Fig. 23 shows the overlaps, pseudo-spin expectation values, and FQHE gap as a function of layer separation d and tunneling strength Δ_{SAS} for several values of charge imbalance tunneling strength $\Delta\rho$. Qualitatively, the overlaps (Fig. 23a and b) are similar in the SLL and LLL. However, comparing them side-by-side, the overlap with the Halperin 331 state achieves a higher value in the LLL than it does in the SLL. The opposite is true for

the overlap with the Moore-Read Pfaffian state where the overlap achieves a higher value in the SLL than it does in the LLL. These differences are manifest even while the pseudo-spin expectation values (Fig. 23c) in the SLL, compared to the LLL, cannot visually be distinguished. Thus, while the values of the Haldane pseudopotentials in the SLL are not different enough from the LLL to change pseudo-spin expectation values, i.e., the system is one-component or two-component at almost exactly the same place in parameter space in both the LLL and SLL, the differences are enough to change the character of the overlaps and the FQHE energy gap.

Fig. 23d shows the FQHE energy gap, and again, there is a marked difference between the result in the LLL versus SLL. Similar to the higher overlap value between the exact ground state and the Moore-Read Pfaffian state in the SLL, the FQHE energy gap has a maximum in the Pf region of the approximate quantum phase diagram especially along the Δ_{SAS} axis for small d . (The opposite is true in the LLL—the FQHE energy gap is largest in the Halperin 331 region of the quantum phase diagram.) We see this behavior also in the wide-quantum-well results.

B. Wide-quantum-well

In Fig. 24 we plot the overlap between the exact ground state of the WQW model and the Moore-Read Pfaffian wavefunction written in the layer-basis (top panel) and *SAS*-basis (lower panel). This figure is, of course, similar to, and should be compared to, Fig. 19 showing the same thing for the bilayer model. Qualitatively, the same behavior is manifest in the two models. As the WQW width W is increased it takes a larger and larger tunneling strength to increase the overlap with the Pf.

The overlap between the ground state and the Halperin 331 state is shown in Fig. 25. Again, we only show the overlap with the Halperin 331 state written in the layer-basis since the overlap with the *SAS*-basis 331 state is almost zero throughout parameter space. The results are qualitatively similar to those of the bilayer model. However, for $W = 2$ (Fig. 25b) there is a slight maximum in the overlap as Δ_{SAS} is increased from zero at $\Delta_{SAS} \sim 0.03$. This is an interesting result that is harder to understand—increasing Δ_{SAS} drives the system to be one-component and one would surmise that increasing this parameter would lower the overlap with the 331 state monotonically. For $W = 4$ we see that two peaks in the overlap appear; one for small values of Δ_{SAS} and another for a larger value with a strong minimum in-between; behavior is particular to the WQW model. Similar to the lowest Landau level, the expectation value of $(N_S - N_{AS})/2$ for $W \geq 2$ is negative for small Δ_{SAS} and $\Delta\rho$. In fact, this negative value means that the system prefers to have more electrons in the *AS* state than the *S* state. However, the system is still more one-component in those regions, such as the region in Fig. 26b along the $\Delta\rho = 0$ axis near $\Delta_{SAS} \sim 0.3$, which correspond to a

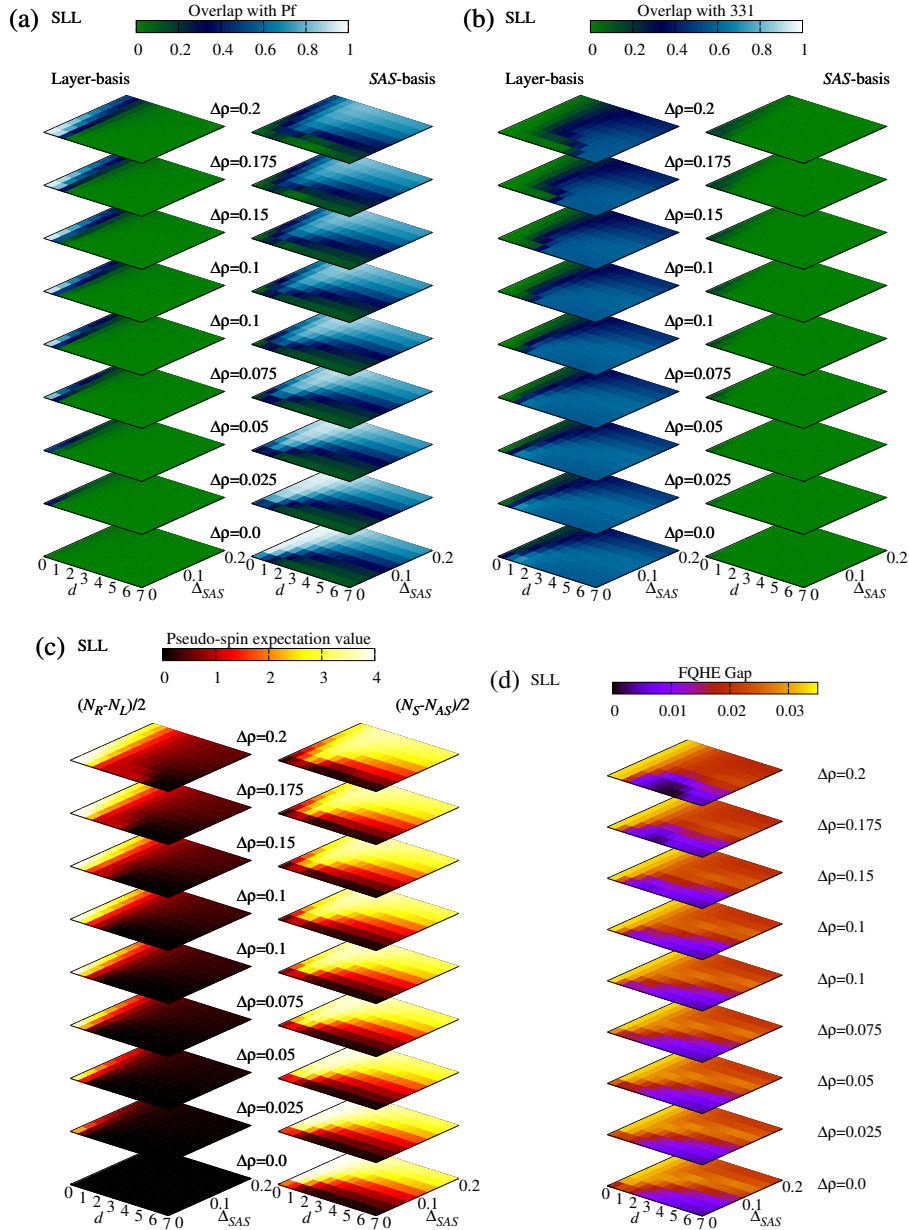


FIG. 23. (Color online) Second Landau level: Same as Fig. 18 except that all plots are shown as a function of inter-layer tunneling Δ_{SAS} and layer separation d for a number of different charge imbalances $\Delta\rho$ and zero individual layer thickness $w = 0$.

maximum in the overlap with the 331 state. At any rate, this behavior marks a qualitative difference between the bilayer and WQW models.

Lastly, we show the FQHE energy gap for $\Delta\rho = 0$ in Fig. 27b along with the overlap between the *SAS*-basis Moore-Read Pfaffian state (top panel of Fig. 27a) and the layer-basis Halperin 331 state (bottom panel of Fig. 27a), respectively. When the FQHE energy gap is non-zero, and the system therefore would be expected to exhibit the FQHE, the overlap with the Pfaffian state is large. On the other hand, in the region of parameter space where the FQHE energy gap is small, the Halperin

331 state has a larger overlap. Thus, independent of our model of choice, the details of the electron-electron interaction in the second Landau level, compared to the lowest Landau level, make a profound difference. In the second Landau level the Pfaffian wavefunction is a good description of the physics when the system is largely one-component. In the lowest Landau level, the Halperin 331 is a good description of the physics when the system is largely two-component.

Note that there is a peak in the FQHE energy gap for $W \sim 2$ and $\Delta_{SAS} \approx 0$ which is well within the Halperin 331 part of the approximate quantum phase diagram.

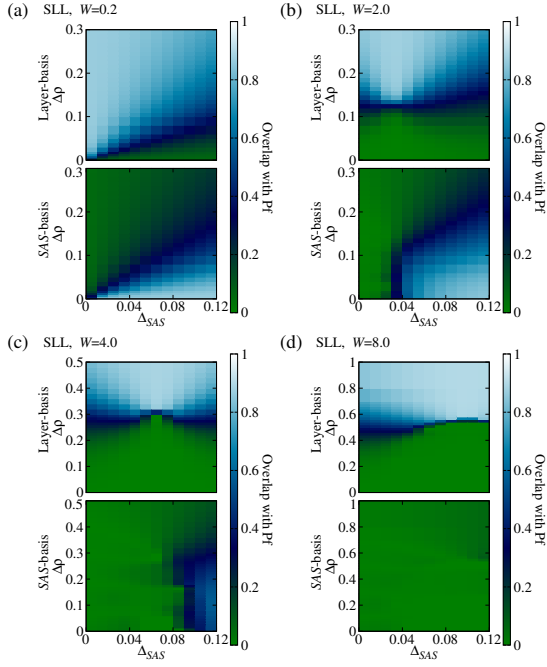


FIG. 24. (Color online) Second Landau level: Wavefunction overlap between the Moore-Read Pfaffian wavefunction in the layer-basis (top panel) and the SAS-basis (lower panel) and the exact ground state for the WQW for (a) $W = 0.2$, (b) $W = 2$, (c) $W = 4$ and (d) $W = 8$ as a function of Δ_{SAS} and $\Delta\rho$.

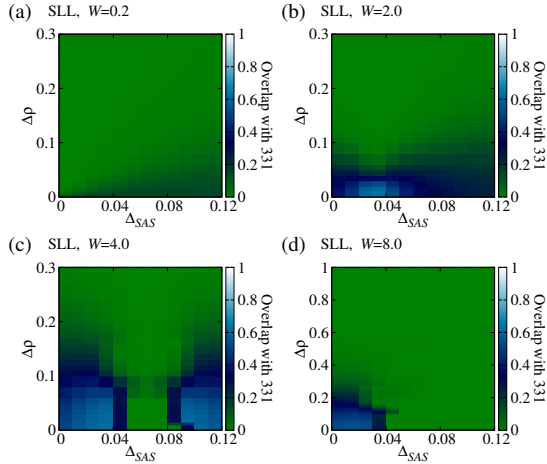


FIG. 25. (Color online) Second Landau level: Wavefunction overlap between the Halperin 331 wavefunction in the layer-basis and the exact ground state for the WQW for (a) $W = 0.2$, (b) $W = 2$, (c) $W = 4$ and (d) $W = 8$ as a function of Δ_{SAS} and $\Delta\rho$. Note that the overlap with the layer-basis Halperin 331 state is not shown since it is always nearly zero.

Even though the overlap with the 331 state is small in that region of parameter space it could correspond to a two-component Abelian FQHE for bilayer systems in the second Landau level at total $\nu = 5/2$ that is in the same universality class as the Halperin 331 state.

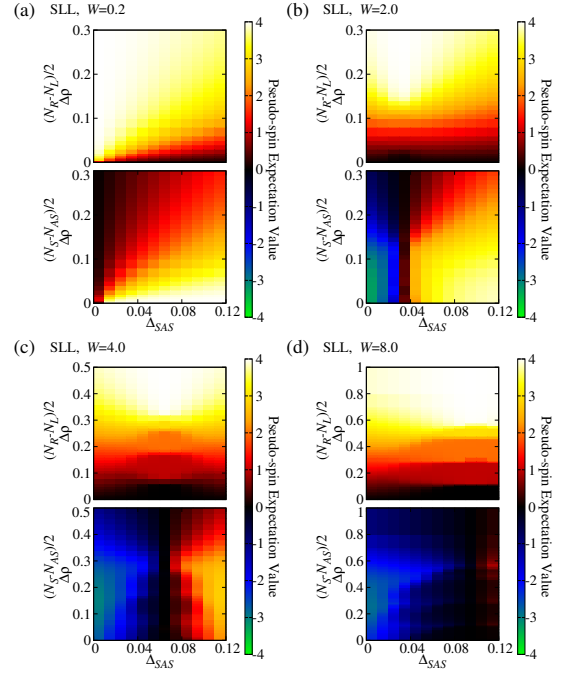


FIG. 26. (Color online) Second Landau level: Pseudo-spin expectation value of the exact ground state (for the WQW model) of $(N_R - N_L)/2$ (top panel) and $(N_S - N_{AS})/2$ (lower panel) for (a) $W = 0.2$, (b) $W = 2$, (c) $W = 4$ and (d) $W = 8$. Note that the WQW model always breaks $SU(2)$ symmetry even for small W and that for $W \geq 2$ there are negative values of $(N_S - N_{AS})/2$ meaning the system prefers, in some regions of parameter space, to have more electrons in the AS state compared to the S state even for positive and non-zero Δ_{SAS} .

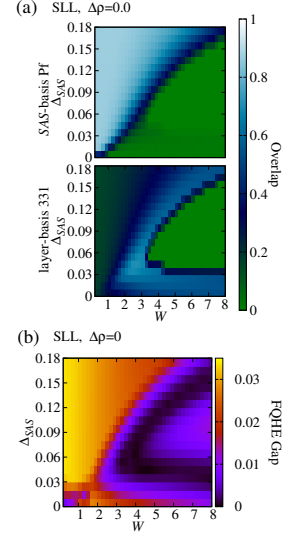


FIG. 27. (Color online) Second Landau level: (b) FQHE energy gap for the WQW model as a function of W and Δ_{SAS} with $\Delta\rho = 0$. Also shown is the (a) overlap between the SAS-basis Moore-Read Pfaffian (top panel) and the layer-basis Halperin 331 (bottom panel) wavefunctions and the exact ground state for $\Delta\rho = 0$.

VI. CONCLUSIONS

In conclusion, we have investigated the FQHE in two-component systems for the half-filled lowest and second Landau levels ($\nu = 1/2$ and $\nu = 5/2$, respectively) as a function of both tunneling strengths; inter-layer tunneling and charge imbalancing. This work was motivated by the recent experimental systems investigated in Refs. 6 and 7.

Our main results are as follows:

(i) The FQHE at $\nu = 1/2$ is described by the (Abelian) Halperin 331 two-component state which is remarkably robust to charge imbalance tunneling. When the system is driven into the one-component region of parameter space, we find that the (non-Abelian) Moore-Read Pfaffian state is most likely beaten out by other competing non-FQHE phases (cf. striped phase or (Composite Fermion) Fermi sea). The reason we suspect this is because even though the overlap between the exact ground state and the Pf (in the *SAS*- or layer-basis, depending on the region of parameter space, i.e., whether Δ_{SAS} is large and $\Delta\rho$ is small or vice-versa) is large, the FQHE energy gap has a peak that is (slightly) on the Halperin 331 side of the approximate quantum phase diagram, where the quantum phase diagram determination is described in Sec. IV. This result, along with recent numerical calculations by Storni *et al.*⁵⁸ (as well as Refs. 61 and 83), leads us to conclude that the one-component $\nu = 1/2$ is likely to be a non-FQHE striped phase or (Composite Fermion) Fermi sea. In the effective BCS description, the increase of tunneling (in the layer-basis) or charge imbalance (in the *SAS*-basis) leads also to the increase of the effective chemical potential of the “even” channel which drives the system into a compressible phase⁸³.

We also find that our calculations are unable to explain the recent results of Shabani *et al.*^{6,7}, which consider *only* the competing Moore-Read Pfaffian and Halperin 331 states. In that work, they observe no FQHE at $\nu = 1/2$ when the charge imbalance is zero, an emerging FQHE at $\nu = 1/2$ for non-zero charge imbalance, and finally, that the FQHE is eventually destroyed upon increasing charge imbalance. While we find that the Halperin 331 FQHE is quite robust to a charge imbalance tunneling term, our results would suggest that the FQHE would monotonically decrease in strength with increasing charge imbalance

(that is, the measured activation gap would decrease in strength, the minimum in R_{xx} would weaken, and/or the “quality” of the plateau in R_{xy} would deteriorate)—we would expect experiments to observe a FQHE at $\nu = 1/2$ with zero charge imbalance that is eventually destroyed upon further imbalancing. The fact that this does not happen in the experiment indicates that the observed state at large imbalance must be something different from the 331 or the Pfaffian state, at least within our model calculations.

(ii) The FQHE in the second Landau level at $\nu = 5/2$ is most likely the spin-polarized and one-component (non-Abelian) Moore-Read Pfaffian state. This state, similar to the Halperin 331 state in the lowest Landau level, is remarkably robust to charge imbalancing. We also find that in regions of parameter space when the system is largely two-component, i.e., for small Δ_{SAS} and $\Delta\rho$, the system might display a FQHE described by the (Abelian) Halperin 331 state. This suggests⁵ the exciting possibility of experimentally tuning parameters to drive an Abelian FQHE state (331) at $\nu = 5/2$ into a non-Abelian FQHE state (Pf) at $\nu = 5/2$ by way of a quantum phase transition.

(iii) One of our surprising theoretical findings is that the Halperin 331 two-component bilayer Abelian paired FQHE is extremely robust, and survives, not only substantial inter-layer tunneling, but also substantial charge imbalance. We suspect that this result is quite general and possibly also applies to other Abelian paired states⁶⁸ in the same universality class of the 331 state.

The physics of the bilayer FQHE at $\nu = 5/2$ is extremely rich with many unanswered and fascination questions (not to mention the fact that the bilayer problem in higher Landau levels is conceptually difficult and non-trivial (see Sec. V)) that, in our opinion, are awaiting experimental answers.

VII. ACKNOWLEDGEMENTS

MRP and SDS are grateful to Microsoft Q for support. ZP was supported by the Serbian Ministry of Science under Grant No. 141035 and by the Agence Nationale de la Recherche under Grant No. ANR-JCJC-0003-01. MRP thanks Vito Scarola for helpful comments. ZP most gratefully acknowledges helpful discussions and former collaboration with M. Goerbig and N. Regnault on setting up the wide-quantum-well model.

¹ S. He, S. Das Sarma, and X. C. Xie, Phys. Rev. B **47**, 4394 (1993).

² S. He, X. C. Xie, S. Das Sarma, and F. C. Zhang, Phys. Rev. B **43**, 9339 (1991).

³ K. Nomura and D. Yoshioka, J. Phys. Soc. Jpn. **73**, 2612 (2004).

⁴ Z. Papić, G. Möller, M. V. Milovanović, N. Regnault, and M. O. Goerbig, Phys. Rev. B **79**, 245325 (2009).

⁵ M. R. Peterson and S. Das Sarma, Phys. Rev. B **81**, 165304 (2010).

⁶ J. Shabani, T. Gokmen, and M. Shayegan, Phys. Rev. Lett. **103**, 046805 (2009).

- ⁷ J. Shabani, T. Gokmen, Y. T. Chiu, and M. Shayegan, Phys. Rev. Lett. **103**, 256802 (2009).
- ⁸ D. C. Tsui, H. L. Stormer, and A. C. Gossard, Phys. Rev. Lett. **48**, 1559 (1982).
- ⁹ R. B. Laughlin, Phys. Rev. Lett. **50**, 1395 (1983).
- ¹⁰ *Perspectives in Quantum Hall Effects*, edited by S. Das Sarma and A. Pinczuk (Wiley, New York, 1997).
- ¹¹ *Composite Fermions: A Unified View of the Quantum Hall Regime*, edited by O. Heinonen (World Scientific, New Jersey, 1998).
- ¹² J. K. Jain, *Composite Fermions* (Cambridge University Press, New York, 2007).
- ¹³ J. K. Jain, Phys. Rev. Lett. **63**, 199 (1989).
- ¹⁴ X. G. Wen and Q. Niu, Phys. Rev. B **41**, 9377 (1990).
- ¹⁵ R. Willett, J. P. Eisenstein, H. L. Stormer, D. C. Tsui, A. C. Gossard, and J. H. English, Phys. Rev. Lett. **59**, 1776 (1987).
- ¹⁶ B. I. Halperin, P. A. Lee, and N. Read, Phys. Rev. B **47**, 7312 (1993).
- ¹⁷ V. Kalmeyer and S.-C. Zhang, Phys. Rev. B **46**, 9889 (1992).
- ¹⁸ E. Rezayi and N. Read, Phys. Rev. Lett. **72**, 900 (1994).
- ¹⁹ R. L. Willett, R. R. Ruel, K. W. West, and L. N. Pfeiffer, Phys. Rev. Lett. **71**, 3846 (1993).
- ²⁰ R. R. Du, H. L. Stormer, D. C. Tsui, L. N. Pfeiffer, and K. W. West, Phys. Rev. Lett. **70**, 2944 (1993).
- ²¹ W. Kang, H. L. Stormer, L. N. Pfeiffer, K. W. Baldwin, and K. W. West, Phys. Rev. Lett. **71**, 3850 (1993).
- ²² J. P. Eisenstein, R. Willett, H. L. Stormer, D. C. Tsui, A. C. Gossard, and J. H. English, Phys. Rev. Lett. **61**, 997 (1988).
- ²³ P. L. Gammel, D. J. Bishop, J. P. Eisenstein, J. H. English, A. C. Gossard, R. Ruel, and H. L. Stormer, Phys. Rev. B **38**, 10128 (1988).
- ²⁴ W. Pan, J.-S. Xia, V. Shvarts, D. E. Adams, H. L. Stormer, D. C. Tsui, L. N. Pfeiffer, K. W. Baldwin, and K. W. West, Phys. Rev. Lett. **83**, 3530 (1999).
- ²⁵ J. P. Eisenstein, K. B. Cooper, L. N. Pfeiffer, and K. W. West, Phys. Rev. Lett. **88**, 076801 (2002).
- ²⁶ J. S. Xia, W. Pan, C. L. Vicente, E. D. Adams, N. S. Sullivan, H. L. Stormer, D. C. Tsui, L. N. Pfeiffer, K. W. Baldwin, and K. W. West, Phys. Rev. Lett. **93**, 176809 (2004).
- ²⁷ G. A. Csáthy, J. S. Xia, C. L. Vicente, E. D. Adams, N. S. Sullivan, H. L. Stormer, D. C. Tsui, L. N. Pfeiffer, and K. W. West, Phys. Rev. Lett. **94**, 146801 (2005).
- ²⁸ H. C. Choi, W. Kang, S. Das Sarma, L. N. Pfeiffer, and K. W. West, Phys. Rev. B **77**, 081301 (2008).
- ²⁹ J. Nuebler, V. Umansky, R. Morf, M. Heiblum, K. von Klitzing, and J. Smet, Phys. Rev. B **81**, 035316 (2010).
- ³⁰ C. R. Dean, B. A. Piot, P. Hayden, S. Das Sarma, G. Gervais, L. N. Pfeiffer, and K. W. West, Phys. Rev. Lett. **101**, 186806 (2008).
- ³¹ S. Das Sarma, G. Gervais and X. Zho, arXiv:1007.1688 (unpublished).
- ³² C. R. Dean, B. A. Piot, P. Hayden, S. D. Sarma, G. Gervais, L. N. Pfeiffer, and K. W. West, Phys. Rev. Lett. **100**, 146803 (2008).
- ³³ C. R. Dean, B. A. Piot, G. Gervais, L. N. Pfeiffer, and K. W. West, Phys. Rev. B **80**, 153301 (2009).
- ³⁴ T. D. Rhone, American Physical Society March Meeting Invited Talk Y2.00003 (unpublished).
- ³⁵ M. Stern, P. Plochocka, V. Umansky, D. K. Maude, M. Potemski, I. Bar-Joseph, arXiv:1005.3112 (unpublished).
- ³⁶ W. Bishara and C. Nayak, Phys. Rev. B **80**, 121302 (2009).
- ³⁷ E. H. Rezayi and S. H. Simon, arXiv:0912.0109 (unpublished).
- ³⁸ A. Wojs, C. Tóke and J. K. Jain, arXiv:1005.4365 (unpublished).
- ³⁹ H. Wang, D. N. Sheng, and F. D. M. Haldane, Phys. Rev. B **80**, 241311 (2009).
- ⁴⁰ W. Pan, H. L. Stormer, D. C. Tsui, L. N. Pfeiffer, K. W. Baldwin, and K. W. West, Solid State Communications **119**, 641 (2001), ISSN 0038-1098.
- ⁴¹ C. Zhang, T. Knuuttila, Y. Dai, R. R. Du, L. N. Pfeiffer, and K. W. West, Phys. Rev. Lett. **104**, 166801 (2010).
- ⁴² R. H. Morf, Phys. Rev. Lett. **80**, 1505 (1998).
- ⁴³ A. E. Feiguin, E. Rezayi, C. Nayak, and S. Das Sarma, Phys. Rev. Lett. **100**, 166803 (2008).
- ⁴⁴ A. Y. Kitaev, Annals of Physics **303**, 2 (2003), ISSN 0003-4916.
- ⁴⁵ C. Nayak, S. H. Simon, A. Stern, M. Freedman, and S. D. Sarma, Rev. Mod. Phys. **80**, 1083 (2008).
- ⁴⁶ G. Moore and N. Read, Nucl. Phys. B **360**, 362 (1991).
- ⁴⁷ S. Das Sarma, M. Freedman, and C. Nayak, Phys. Rev. Lett. **94**, 166802 (2005).
- ⁴⁸ J. Bardeen, L. N. Cooper, and J. R. Schrieffer, Phys. Rev. **106**, 162 (1957).
- ⁴⁹ J. Bardeen, L. N. Cooper, and J. R. Schrieffer, Phys. Rev. **108**, 1175 (1957).
- ⁵⁰ N. Read and D. Green, Phys. Rev. B **61**, 10267 (2000).
- ⁵¹ S.-S. Lee, S. Ryu, C. Nayak, and M. P. A. Fisher, Phys. Rev. Lett. **99**, 236807 (2007).
- ⁵² M. Levin, B. I. Halperin, and B. Rosenow, Phys. Rev. Lett. **99**, 236806 (2007).
- ⁵³ M. R. Peterson, K. Park, and S. Das Sarma, Phys. Rev. Lett. **101**, 156803 (2008).
- ⁵⁴ N. d'Ambrumenil and A. M. Reynolds, Journal of Physics C: Solid State Physics **21**, 119 (1988).
- ⁵⁵ A. H. MacDonald, Phys. Rev. B **30**, 3550 (1984).
- ⁵⁶ V. W. Scarola, K. Park, and J. K. Jain, Phys. Rev. B **62**, R16259 (2000).
- ⁵⁷ C. Tóke, M. R. Peterson, G. S. Jeon, and J. K. Jain, Phys. Rev. B **72**, 125315 (2005).
- ⁵⁸ M. Storni, R. H. Morf, and S. Das Sarma, Phys. Rev. Lett. **104**, 076803 (2010).
- ⁵⁹ M. R. Peterson, T. Jolicœur, and S. D. Sarma, Phys. Rev. Lett. **101**, 016807 (2008).
- ⁶⁰ M. R. Peterson, T. Jolicœur, and S. D. Sarma, Phys. Rev. B **78**, 155308 (2008).
- ⁶¹ Z. Papić, N. Regnault, and S. Das Sarma, Phys. Rev. B **80**, 201303 (2009).
- ⁶² Y. W. Suen, L. W. Engel, M. B. Santos, M. Shayegan, and D. C. Tsui, Phys. Rev. Lett. **68**, 1379 (1992).
- ⁶³ Y. W. Suen, M. B. Santos, and M. Shayegan, Phys. Rev. Lett. **69**, 3551 (1992).
- ⁶⁴ Y. W. Suen, H. C. Manoharan, X. Ying, M. B. Santos, and M. Shayegan, Phys. Rev. Lett. **72**, 3405 (1994).
- ⁶⁵ J. P. Eisenstein, G. S. Boebinger, L. N. Pfeiffer, K. W. West, and S. He, Phys. Rev. Lett. **68**, 1383 (1992).
- ⁶⁶ B. I. Halperin, Helv. Phys. Acta **56**, 783 (1983).
- ⁶⁷ D. R. Luhman, W. Pan, D. C. Tsui, L. N. Pfeiffer, K. W. Baldwin, and K. W. West, Phys. Rev. Lett. **101**, 266804 (2008).
- ⁶⁸ V. W. Scarola and J. K. Jain, Phys. Rev. B **64**, 085313 (2001).
- ⁶⁹ V. W. Scarola, C. May, M. R. Peterson, and M. Troyer, arXiv:1004.1636 (unpublished).

- ⁷⁰ F. C. Zhang and S. Das Sarma, Phys. Rev. B **33**, 2903 (1986).
- ⁷¹ A. H. MacDonald, P. M. Platzman, and G. S. Boebinger, Phys. Rev. Lett. **65**, 775 (1990).
- ⁷² J. Schliemann, S. M. Girvin, and A. H. MacDonald, Phys. Rev. Lett. **86**, 1849 (2001).
- ⁷³ K. Nomura and D. Yoshioka, Phys. Rev. B **66**, 153310 (2002).
- ⁷⁴ K. Park, Phys. Rev. B **69**, 045319 (2004).
- ⁷⁵ S. H. Simon, E. H. Rezayi, and M. V. Milovanovic, Phys. Rev. Lett. **91**, 046803 (2003).
- ⁷⁶ G. Möller, S. H. Simon, and E. H. Rezayi, Phys. Rev. Lett. **101**, 176803 (2008).
- ⁷⁷ G. Möller, S. H. Simon, and E. H. Rezayi, Phys. Rev. B **79**, 125106 (2009).
- ⁷⁸ See J. R. Schrieffer, *Theory of Superconductivity* (Addison-Wesley, Reading, MA, 1964) and Ref. 50 for a discussion of the Pfaffian form of the real space BCS pairing wavefunction.
- ⁷⁹ M. Milovanovi and N. Read, Phys. Rev. B **53**, 13559 (1996).
- ⁸⁰ E. H. Rezayi and F. D. M. Haldane, Phys. Rev. Lett. **84**, 4685 (2000).
- ⁸¹ F. D. M. Haldane, Phys. Rev. Lett. **51**, 605 (1983).
- ⁸² T. T. Yang and C. N. Yang, Nucl. Phys. B **107**, 365 (1976).
- ⁸³ Z. Papić, M. O. Goerbig, N. Regnault and M. V. Milovanović, arXiv:0912.3103 (unpublished).
- ⁸⁴ D. Yoshioka, B. I. Halperin, and P. A. Lee, Phys. Rev. Lett. **50**, 1219 (1983).
- ⁸⁵ D. Yoshioka, Phys. Rev. B **29**, 6833 (1984).
- ⁸⁶ F. D. M. Haldane, Phys. Rev. Lett. **55**, 2095 (1985).
- ⁸⁷ X.-G. Wen and A. Zee, Phys. Rev. B **58**, 15717 (1998).
- ⁸⁸ N. Read and E. Rezayi, Phys. Rev. B **54**, 16864 (1996).
- ⁸⁹ C. Shi, S. Jolad, N. Regnault, and J. K. Jain, Phys. Rev. B **77**, 155127 (2008).
- ⁹⁰ G. Möller and S. H. Simon, Phys. Rev. B **77**, 075319 (2008).